Title:

Brain composition in *Heliconius* butterflies, post-eclosion growth and experience dependent neuropil plasticity

Authors:

Stephen H. Montgomery[1], Richard M. Merrill[2,3], Swidbert R. Ott[4]

Institutional affiliations:

[1] Dept. Genetics, Evolution & Environment, University College London, Gower Street, London, UK, WC1E 6BT

[2] Dept. Zoology, University of Cambridge, Downing Street, Cambridge, UK, CB2 3EJ

[3] Smithsonian Tropical Research Institute, MRC 0580-12, Unit 9100 Box 0948, DPO AA 34002-9998, Panama

[4] Dept. Biology, University of Leicester, Adrian Building, University Road, Leicester, UK, LE1 7RH

Corresponding author: Stephen H. Montgomery: Stephen.Montgomery@cantab.net

Running head: *Anatomy and plasticity of* Heliconius *brains*

Key words: adaptive brain evolution, comparative neuroanatomy, *Heliconius*, Lepidoptera, mushroom bodies, plasticity

Financial support: This research was supported by research fellowships from the Royal Commission of the Exhibition of 1851 and Leverhulme Trust, a Royal Society Research Grant (RG110466) and a British Ecological Society Early Career Project Grant awarded to SHM. RMM was supported by a Junior Research Fellowship from King's College, Cambridge and an Ernyst Mayr Fellowship from STRI. SRO was supported by a University Research Fellowship from the Royal Society, London (UK).

ABSTRACT

Behavioral and sensory adaptations are often based in the differential expansion of brain components. These volumetric differences represent differences in investment, processing capacity and/or connectivity, and can be used to investigate functional and evolutionary relationships between different brain regions. Here, we describe the brain composition of two species of *Heliconius* butterflies, a long-standing study system for investigating ecological adaptation and speciation. We confirm a previous report of striking mushroom body expansion, and explore patterns of post-eclosion growth and experience-dependent plasticity in neural development. This analysis uncovers two phases of post-emergence mushroom body growth comparable to those of foraging hymenoptera, but also identifies plasticity in several other neuropil. An interspecific analysis suggests *Heliconius* may display remarkable levels of investment in mushroom bodies for a Lepidopteran, and indeed rank highly compared to other insects. We also describe patterns of adaptive divergence in the volume of both peripheral and central neuropil within *Heliconius*, and across Lepidoptera, that suggest changes in brain composition plays an important role in ecological adaptation. Our analyses lay the foundation for future comparative and experimental analyses that will establish *Heliconius* as a useful case study in evolutionary neurobiology.

INTRODUCTION

Behavioral adaptations can allow populations to respond to environmental change and to invade new ecological niches. These behavioral changes are largely based in adaptive changes in brain function, which may in turn involve changes in the size and macro-structure of the brain (e.g., Gonda et al., 2009a,b, 2013; Park and Bell, 2010). For example, a clear signature of adaptive, phylogenetic divergence in brain composition in response to ecological variation is seen within many invertebrate and vertebrate species in their sensory neuropil (e.g. Barton et al., 1995; Huber et al., 1997; Gronenberg and Hölldobler, 1999; O'Donnell et al., 2013; Montgomery and Ott, 2015). In this case, nocturnal species, or those occupying low light environments, tend to have larger olfactory neuropil, and smaller visual neuropil (Barton et al., 1995; Montgomery and Ott, 2015).

Beyond the primary sensory regions, ecological selection pressures may have diverse effects on higher brain centers. The complexity of the physical (Capaldi et al., 1999; Safi and Dechmann, 2005; Pollen et al., 2007; Shumway, 2008; Farris and Schulmeister, 2011) or social environment (Barton and Dunbar, 1997; Burish et al., 2004; Lihoreau et al., 2012) have a detectable influence in shaping brain size and structure. For example, in vertebrates, this is clearly manifest in an evolutionary association between the need for spatial memory and the volume of the hippocampus (Clayton and Krebs, 1995; Garamszegi and Eens, 2004). In insects a similar association is found with the mushroom bodies (Farris and Schulmeister, 2011).

Differential expansions of individual brain structures shed light not only on species-specific biology and neuroecology, but more generally on the functional relationships between brain components (Barton and Harvey, 2000; Whiting and Barton, 2003), the relative strength of developmental constraints (Finlay and Darlington, 1995; Barton and Harvey, 2000), and on how very different brains produce seemingly similarly complex behavior (Giurfa and Menzel, 2001; Chittka and Niven, 2009; Farris, 2013).

Given their longstanding role in studies of both adaptation and brain function, the Lepidoptera are perhaps an underutilized group for integrating these fields to investigate evolutionary neurobiology. The Neotropical genus *Heliconius* (Heliconiinae, Nymphalidae) is well known for its diversity of bright warning patterns

that are often involved in Müllerian mimicry, where two or more unpalatable species converge on the same warning-signal to more efficiently advertise their distastefulness to predators (Müller, 1879; Mallet & Barton 1989; Merrill et al 2013). Perhaps as a result these butterflies have been intensively studied, leading to insights into a range of areas including population and community ecology, evolutionary genetics and development, as well as more generally contributing to our understanding of adaptation and speciation (Merrill et al., 2015).

Heliconius display a strong pattern of ecological divergence (Boggs et al., 1981; Estrada and Jiggins, 2002; Jiggins, 2008), and a number of striking behavioral adaptations (Gilbert, 1972, 1975; Mallet, 1986). Chief among these is a dietary adaptation, unique among Lepidoptera; adult pollen feeding (Gilbert, 1972, 1975). With the exception of four species formerly ascribed to the genus *Neruda* (Beltrán et al., 2007; Kozak et al., 2015), all *Heliconius* actively collect and ingest pollen as adults. This provides a rich source of amino acids and permits a greatly extended lifespan of up to six months without reproductive senescence, and shifts the energetic costs of chemical defense to larvae (Gilbert, 1972; Benson, 1972; Ehrlich and Gilbert, 1973; Dunlap-Pianka et al., 1977; Cardoso and Gilbert, 2013). Without access to pollen *Heliconius* suffer a major reduction in longevity and reproductive success (Gilbert, 1972; Dunlap-Pianka et al., 1977; O'Brien et al., 2003).

Adult *Heliconius* collect pollen from a relatively restricted range of mostly Cucurbitaceous plants (Estrada and Jiggins, 2002), which are spatially dispersed and occur at low densities (Gilbert, 1975). Several lines of evidence suggest selection for pollen feeding has shaped *Heliconius* foraging behavior. Individuals inhabit home ranges of typically less than 1 km^2, within which individuals repeatedly utilize a small number of roosting sites that they return to with high fidelity (Turner, 1971; Benson, 1972; Gilbert, 1975; Mallet, 1986; Murawski and Gilbert, 1986; Finkbeiner, 2014). On leaving the roost individuals visit feeding sites with a level of consistency in time and space that strongly suggests 'trap-lining' behavior (Ehrlich and Gilbert, 1973; Gilbert, 1975, 1993; Mallet, 1986), analogous to that observed in foraging bees (Janzen, 1971; Heinrich, 1979). Roosts themselves are located visually (Jones, 1930; Gilbert, 1972; Ehrlich and Gilbert, 1973; Mallet, 1986), and older individuals tend to be more efficient foragers (Boggs et al., 1981; Gilbert, 1993). Together these observations suggest the evolution of pollen feeding in *Heliconius* was facilitated by

an enhanced, visually-orientated ‘circadian memory’ that utilizes visual landmarks (Gilbert, 1975).

The evolution of this behavior must involve “some elaboration of the nervous system” (Turner, 1981), suggested to lie in the mushroom bodies (Sivinski, 1989). Sivinski (1989) reported that the percentage of the brain occupied by the mushroom body in two individuals of *Heliconius charithonia* was 3–4 times larger than in six other species of butterfly, including two non-pollen feeding Heliconiini. In other insects, mushroom body expansion has been associated with increased demands for higher order information processing, either in relation to social ecology or foraging behavior, both within and between species (Dujardin, 1859; Withers et al., 1993, 2008; Gronenberg et al., 1996; Ehmer and Ron, 1999; Molina and O’Donnell, 2007; Smith et al., 2010; O’Donnell et al., 2013; Gronenberg et al., 1996; Fahrbach et al., 2003; Farris and Roberts, 2005; Farris and Schulmeister, 2011).

Mushroom bodies have a variety of roles in olfactory associative learning, sensory integration, filtering and attention (Zars, 2000; Farris, 2005, 2013; Menzel, 2014). Direct experimental evidence also links mushroom body function with spatial learning and memory in some, but not all, insects (Mizunami et al., 1998; Neuser et al., 2008; Ofstad et al., 2011). Comparisons across species suggest that extreme evolutionary expansion of the mushroom body is commonly associated with changes in foraging behavior that depend on spatial memory or the complexity of sensory information utilized by the species (Farris, 2005, 2013). For example, in Hymenoptera, mushroom body expansion coincides with the origin of parasitoidism (Farris and Schulmeister, 2011), a dietary adaptation that involves place-centered foraging and spatial memory for host location (Rosenheim, 1987; van Nouhuys and Kaartinen, 2008).

Patterns of ontogenetic neuropil plasticity in trap-lining insects, such as the honeybee, *Apis mellifera*, further link foraging behavior and the mushroom bodies (Withers et al., 1993; Durst et al., 1994; Capaldi et al., 1999; Farris et al., 2001). Honeybees show two forms of post-eclosion growth in mushroom body volume; age dependent growth, which occurs regardless of environmental variation, and experience dependent growth which increases with foraging or social experience (Withers et al., 1993; Durst et al., 1994; Fahrbach et al., 1998, 2003; Farris et al., 2001; Maleszka et al., 2009). A similar pattern is found in other Hymenoptera, and there is an intriguing correspondence between the rate and timing of mushroom body

growth and the onset of foraging behavior (Gronenberg et al., 1996; Kühn-Bühlmann and Wehner, 2006; Withers et al., 2008; Jones et al., 2013). These combined growth processes involve substantial volumetric changes, typically 20–30% increases from emergence to maturity (Gronenberg et al., 1996; Fahrbach et al., 1998; Jones et al., 2013), which most probably have strong biological and behavioral significance. Age and environmental effects on neuropil growth are also found in some other central and peripheral neuropil (Gronenberg et al., 1996; Jones et al., 2013).Whether *Heliconius* show similar ontogenetic profiles or experience dependent plasticity in mushroom body growth, as might be predicted if they are involved in spatial memory, is not known.

Assessing levels of environment dependent neurological plasticity may provide insights into the role behavior may have played during the *Heliconius* radiation, and during speciation in general (Pfennig et al., 2010; Snell-Rood, 2013). Speciation in *Heliconius* is thought to frequently mimetic shifts associated with habitat divergence (Mallet, 1993; Jiggins, 2008). Different mimicry rings represent alternative adaptive peaks, and may be associated with variation in predator communities, interspecific competition, habitat structure and/or light environment (Smiley, 1978; Mallet, 1993; Estrada and Jiggins, 2002; Merrill et al 2013). Consequently, shifts in mimetic resemblance may impose extensive secondary selection for behavioral adaptations. Indeed, several parapatric sister-species occur along habitat gradients (Jiggins et al., 1996; Estrada and Jiggins, 2002; Arias et al., 2008), supporting evidence that different mimicry rings are ecologically separated (Smiley, 1978; Boggs et al., 1981; Estrada and Jiggins, 2002). A potential role for neural plasticity is established in some cases of recent ecological divergence and adaptation (e.g Gonda et al., 2009a; b, 2013; Park and Bell, 2010). Whether habitat-shifts during the early stages of speciation in *Heliconius* are facilitated by behavioral and neurological plasticity is unknown but of considerable interest (Merrill et al., 2015).

In the current analysis we begin to investigate these topics. We first revisit *Heliconius* brain composition to confirm Sivinksi's (1989) observation that they are greatly expanded. We then compare brain composition between recently emerged insectary-reared individuals, aged insectary-reared individuals, and wild-caught individuals to address several key questions: i) how big are *Heliconius* mushroom bodies? ii) how does their morphology compare with other trap-line foragers? iii) do they have post-eclosion growth patterns comparable to other trap-line foragers? and

iv) is such environmentally induced plasticity present in, or restricted to, the mushroom bodies? These intra-specific comparisons lay the groundwork for comparative analyses across Heliconiini examining the origin and timing of mushroom body expansion. In the meantime, we compare the relative investment in different neuropil in two species of *Heliconius*, *H. erato* and *H. hecale* to each other, and to other Lepidoptera to explore how selection has shaped overall brain composition.

MATERIALS & METHODS

Animals

We collected individuals of two species of *Heliconius*, *H. hecale melicerta* and *H. erato demophoon*. *H. hecale* is generally found in tall forest throughout central America and the Amazon basin, whilst *H. erato* is a widespread forest edge specialist (Brown, 1981). Wild individuals were collected from Gamboa (9°7.4′ N, 79°42.2′ W, elevation 60 m) and the nearby Soberanía National Park, República de Panamá. At this locality *H. hecale* belongs to the 'tiger pattern' mimicry ring, whilst *H. erato* belongs to the 'postman' mimicry ring which are at least partially segregated by habitat preference (Estrada and Jiggins, 2002). Five males and five females of each species were sampled from the wild. We assume all wild-caught individuals were sexually mature, and that the age range is not biased between species or sexes.

Wild individuals were compared with individuals from first or second-generation insectary-reared stock populations, descended from wild caught parents from the same sampling localities. Stock populations were kept in controlled conditions in cages (approximately 1 × 2 × 2 m) of mixed sex at roughly equal densities. Cages were housed at the *Heliconius* insectaries at the Smithsonian Tropical Research Institute's (STRI) facility in Gamboa (see: www.heliconius.org/resources/research-facility). Stocks had access to their preferred host plant (*Passiflora biflora* and *P. vitifolia* respectively for *H. erato* and *H. hecale*), a pollen source (*Psychotria elata*) and feeders containing c. 20% sugar solution with an additional bee-pollen supplement to ensure there was a pollen excess. Larvae were allowed to feed naturally on the host plant.

After emergence from the pupae insectary-reared individuals were collected for two age groups, a recently emerged ‘young’ group (1–3 days post emergence) and an ‘old’ group (2–3 weeks post emergence). *Heliconius* are generally considered to undergo a “callow” period of general inactivity immediately after emergence that lasts about 5 days, during which flight behavior is weak and males are sexually inactive (Mallet, 1980). These age groups therefore represent behaviorally immature and mature individuals. In *Bombus impatiens*, which has a comparable lifespan to *Heliconius* (Plath, 1934; Benson, 1972; Ehrlich and Gilbert, 1973), age-related growth plateaus after c. 10 days (Jones et al., 2013). If *Heliconius* have a comparable developmental trajectory we would expect growth to have reached a plateau in the old group. For *H. hecale* 5 males and 5 females were sampled for both age groups, in *H. erato* 4 males and 6 females were sampled for the ‘young’ group and 5 males and 4 females were sampled for the ‘old’ group. For samples where it was possible to measure the exact time of emergence, there is no significant difference between *H. hecale* and *H. erato* in age structure of the old (*H. erato*: mean = 22.6 days, SD = 8.6; *H. hecale*: mean = 26.4 days, SD = 5.5; t_{13} = -0.899, p = 0.385) or young (*H. erato*: mean = 1.7 days, SD = 0.8; *H. hecale*: mean = 1.3 days, SD = 1.1; t_{17} = 0.829, p = 0.419) insectary-reared groups.

We took three body size measurements for each individual: body mass, weighted to 0.01 g using a OHAUS "Gold Pocket" pocket balance (model YA102); and body length and wingspan, measured using FreeLOGIX 6 inch digital calipers. Wings were kept as voucher specimens in glassine envelopes. Samples were collected and exported under permits SEX/A-3-12 and SE/A-7-13 obtained from the Autoridad Nacional del Ambiente, República de Panamá in conjunction with STRI.

Antibodies and sera for neuropil staining

We used indirect immunofluorescence staining against synapsin to reveal the neuropil structure of the brain under a confocal microscope (Ott, 2008). This technique exploits the abundant expression of synapsin, a vesicle-associated protein, at presynaptic sites. Monoclonal mouse anti-synapsin antibody 3C11 (anti-SYNORF1; (Klagges et al., 1996) was obtained from the Developmental Studies Hybridoma Bank (DSHB), University of Iowa, Department of Biological Sciences, Iowa City, IA 52242, USA (RRID: AB_2315424). The 3C11 antibody was raised against a bacterially expressed fusion protein generated by adding a glutathione S-transferase

(GST)-tag to a cDNA comprising most of the 5´ open reading frame 1 of the *Drosophila melanogaster* synapsin gene (*Syn*, CG3985). The binding specificity of this antibody was characterised in *D. melanogaster* (Klagges et al., 1996). The epitope was later narrowed down to within LFGGMEVCGL in the C domain (Hofbauer et al., 2009). Bioinformatic analysis has confirmed the presence of this motif in Lepidopteran genomes, and demonstrated that it is highly conserved across Lepidoptera (Montgomery and Ott, 2015). 3C11 immunostaining has been used as an anatomical marker of synaptic neuropil in a wide range of arthropod species including several Lepidoptera: *Danaus plexippus* (Heinze and Reppert, 2012), *Godyris zavaleta* (Montgomery and Ott, 2015) *Heliothis virescens* (Kvello et al., 2009) and *Manduca sexta* (El Jundi et al., 2009b). The staining pattern obtained with 3C11 in the present analysis is similar to other Lepidoptera. Cy2-conjugated affinity-purified polyclonal goat anti-mouse IgG (H+L) antibody (Jackson ImmunoResearch Laboratories, West Grove, PA) was obtained from Stratech Scientific Ltd., Newmarket, Suffolk, UK (Jackson ImmunoResearch Cat No. 115-225-146, RRID: AB_2307343).

Immunocytochemistry

Brains were fixed and stained following a published protocol (Ott, 2008) previously applied to a range of invertebrates including the Monarch butterfly, *D. plexippus* (Heinze and Reppert, 2012), and the Zavaleta Glasswing, *G.* (Montgomery and Ott, 2015). The protocol was divided into two stages, the first of which was performed at the STRI Gamboa Field Station. Briefly, the brain was exposed under HEPES-buffered saline (HBS; 150 mM NaCl; 5 mM KCl; 5 mM $CaCl_2$; 25 mM sucrose; 10 mM HEPES; pH 7.4) and fixed in situ for 16–20 hours at room temperature (RT) in zinc-formaldehyde solution (ZnFA; 0.25% (18.4 mM) $ZnCl_2$; 0.788% (135 mM) NaCl; 1.2% (35 mM) sucrose; 1% formaldehyde) under agitation. Fixation with ZnFA affords considerably better antibody penetration, staining intensity and preservation of morphology than conventional (para)formaldehyde fixation (Ott, 2008; Heinze and Reppert, 2012). The brain was subsequently dissected out, under HBS, by removing the eye cuticle in slices before gently plucking away the main body of the ommatidia and the basement membrane. After removing any surrounding material, the brain was lifted from the head capsule, washed 3 × in HBS and placed into 80% methanol/20% DMSO for a minimum of 2 hours under agitation. The brain was then transferred to

100% methanol and stored at RT. After transportation back to the UK samples were stored at -20˚C.

In the second stage of the protocol, performed in laboratory conditions in the UK, the samples were brought to RT and rehydrated in a decreasing methanol series (90%, 70%, 50%, 30%, 0% in 0.1 M Tris buffer, pH 7.4, 10 minutes each). Normal goat serum (NGS; New England BioLabs, Hitchin, Hertfordshire, UK) and antibodies were diluted in 0.1 M phosphate-buffered saline (PBS; pH 7.4) containing 1% DMSO and 0.005% NaN_3 (PBSd). Non-specific antibody binding was blocked by pre-incubation in 5% NGS (PBSd-NGS) for 2 hours at RT. Antibody 3C11 was then applied at a 1:30 dilution in PBSd-NGS for 3.5 days at 4˚C under agitation. The brains were rinsed in PBSd for 3 × 2 hours before applying the Cy2-conjugated anti-mouse antibody 1:100 in PBSd-NGS for 2.5 days at 4˚C under agitation. This was followed by a series of increasing concentrations (1%, 2%, 4% for 2 hours each, 8%, 15%, 30%, 50%, 60%, 70% and 80% for 1 hour each) of glycerol in 0.1 M Tris buffer with DMSO to 1%. The brains were then passed in a drop of 80% glycerol directly into 100% ethanol and agitated for 30 minutes; the ethanol was changed three times with 30-minute incubations. Finally, to clear the tissue, the ethanol was underlain with methyl salicylate, the brain was allowed to sink, before the methyl salicylate was refreshed twice with 30 minute incubations.

Confocal imaging

Samples were mounted in fresh methyl salicylate between two round cover slips separated by a thin metal washer (UK size M8 or M10). All imaging was performed on a confocal laser-scanning microscope (Leica TCS SP8, Leica Microsystem, Mannheim, Germany) at the University College London Imaging Facility, using a 10× dry objective lens with a numerical aperture of 0.4 (Leica Material No. 11506511, Leica Microsystem, Mannheim, Germany). For each individual brain we captured a series of overlapping stacks using a mechanical *z*-step of 2 μm with an *x*-*y* resolution of 512 × 512 pixels. Imaging the whole brain required 3×2 stacks in the *x*-*y* dimensions with an overlap of 20%. Tiled stacks were automatically merged in Leica Applications Suite Advanced Fluorescence software. Each brain was scanned from the posterior and anterior side to span the full *z*-dimension of the brain. These two image stacks were subsequently merged in Amira 3D analysis software 5.5 (FEI

Visualization Sciences Group), using a custom module 'Advanced Merge' which aligns images using affine registration and subsequently merges to produce the combined stacks. We manually optimized the re-sampling procedure from anterior and posterior stacks for each individual. Finally, to correct for the artifactually shortened *z*-dimension associated with the 10× air objective, a correction factor of 1.52 was applied to the voxel size in the *z*-dimension (Heinze and Reppert, 2012a; Montgomery and Ott, 2015). Images presented in the figures to illustrate key morphological details were captured separately as single confocal sections with an *x*-*y* resolution of 1024 × 1024 pixels.

Neuropil segmentations and volumetric reconstructions

Neuropils were reconstructed from the confocal image stacks in Amira 5.5. We assigned image regions to anatomical structures in the Amira *labelfield* module by defining outlines based on the brightness of the synapsin immunofluorescence. This process segments the image into regions that are assigned to each particular structure, and regions that are not. Within each stack, every forth or fifth image was manually segmented using the outline or magic-wand tool. The segmentation was then interpolated in the *z*-dimension across all images that contain the neuropil of interest before being fine-edited and smoothed in all three dimensions. The *measure statistics* module was used to determine volumes (in μm^3) for each neuropil. 3D polygonal surface models of the neuropils were constructed from the smoothed labelfield outlines using the *SurfaceGen* module. The color code used for the neuropils in the 3D models is consistent with previous neuroanatomical studies of invertebrate brains (Brandt et al., 2005; Kurylas et al., 2008; El Jundi et al., 2009a, b; Dreyer et al., 2010; Heinze and Reppert, 2012; Montgomery and Ott, 2015).

The whole-brain composite stacks were used to reconstruct and measure six paired neuropils in the optic lobes, and seven paired and two unpaired neuropils in the midbrain. All paired neuropils were measured on both sides of the brain in wild-caught individuals to permit tests of asymmetry, yielding two paired measurements per brain (*i.e.*, $N = 10 \times 2$) for each structure. We found no evidence of volumetric asymmetry for either species ($p > 0.05$ for each neuropil in a paired t-tests) and therefore summed the volumes of paired neuropil to calculate the total volume of that structure. In insectary-reared individuals we therefore subsequently measured the

volume of paired neuropil from one hemisphere, chosen at random, and multiplied the measured volume by two to obtain an estimate of total volume of that neuropil. Finally, we measured the total neuropil volume of the midbrain to permit statistical analyses that control for allometric differences. In keeping with the earlier Lepidopteran literature, we use the term 'midbrain' for the fused central mass that comprises of the protocerebral neuromere excluding the optic lobes, the deuto- and tritocerebral neuromeres, and the sub-esophageal neuromeres. For the following statistical analyses we analyzed the central body as a single structure, and summed the volumes of the mushroom body lobes and peduncles as the boundary between these structures was not always clear.

Intraspecific statistical analyses

In all statistical analyses continuous variables were $\log_{10}$-transformed to meet assumptions of normality. Unpaired two-tailed two-sample *t*-tests were used to test for volumetric differences between sexes or groups. We found no robust evidence of sexual dimorphism in neuropil volume of wild caught individuals that could not be explained by allometric scaling and therefore combined male and female data. However, we note that our sample size for each sex is unlikely to be sufficient to provide conclusive support either for or against sexual dimorphism.

Our analyses focused on two intra-specific comparisons: i) we compared 'young' and 'old' insectary-reared individuals and interpret significant differences as evidence for post-eclosion growth or delayed maturation; and ii) we compared wild-caught individuals with 'old' insectary-reared individuals and interpret significant differences as evidence for environmentally induced, experience dependent plasticity. These comparisons were made by estimating the allometric relationship with a measure of overall brain size for each neuropil. The standard allometric scaling relationship can be modeled as $\log(y) = \beta[\log(x)] + \alpha$. We used standard major axis regressions in the SMATR 3 package (Warton et al., 2012) to test for significant shifts in the allometric scaling parameter (β) or the y-intercept (α). To permit comparisons between neuropil, a consistent independent variable was used throughout the analyses that accounts for allometric scaling with total brain size. This was the total volume of the midbrain minus the combined volume of all segmented neuropil in the midbrain, referred to as 'rest of midbrain' (rMid).

Significant differences in β suggest the proportional increase in the dependent variable with size differs between groups, i.e. the slopes are significantly different. The *slope.com* function in SMATR calculates a likelihood ratio statistic for the absence of a common slope, χ^2 distributed with one degree of freedom. Where we identified no heterogeneity in the allometric scaling parameter (β) we performed two further tests. First, we tested for significant differences in α that suggest discrete 'grade-shifts' in the relationship between two variables. The *elev.com* function in SMATR calculates a Wald statistic for the absence of shifts along the y-axis, χ^2 distributed with one degree of freedom. Second, we tested for major axis-shifts along a common slope. This is indicative of co-ordinated changes in the size of the dependent and independent variable between groups. The *shift.com* function in SMATR calculates a Wald statistic for the absence of a shift along a common axis, χ^2 distributed with one degree of freedom. For this test, when significant, we also report the fitted axis (FA) mean that describes the mean position of the group on the common fitted axis. For all statistically significant tests we also present the effect size, measured by the correlation coefficient (r). Effect sizes of $0.1<r<0.3$ are interpreted as 'small' effects, $0.3<r<0.5$ 'medium' effects, and $r<0.5$ 'large' effects (Cohen, 1988).

Patterns of brain:body allometry were explored in a similar manner, using total neuropil volume as the dependent variable (summed volumes of all neuropil in the optic lobes plus the total midbrain volume), and comparing the results obtained using alternative body size measurements as the independent variable. Body mass varies with body condition and reproductive state, we therefore anticipated that body length may be a more reliable way of assessing the allometric relationship between brain and body size in wild caught individuals.

We complemented these analyses with a multivariate analysis of all segmented neuropil volumes and the unsegmented midbrain volume using Discrimant Function Analysis (DFA) to test how reliably individuals can be assigned to their respective groups on the basis of their volumetric differences in neuropil. In this analysis, as well as providing a percentage of correctly assigned individuals, Wilks' lambda provides a measure of the proportion of total variance not explained by group differences, and the χ^2 statistic provides a test for significant group differences. All statistical analyses were performed in R (R Development Core Team, 2008), using the

standard *stats* and *smatr* package, except for the DFA, which was performed in SPSS v. 22 for OS X (SPSS Inc., Chicago, IL)

Interspecific statistical analyses

An examination of allometric scaling was also applied to interspecific analyses between *H. hecale* and *H. erato* to test for species differences in brain composition. We compared both wild-caught and 'old' insectary-reared individuals. Where significant species differences are found in wild caught individuals but not 'old' insectary-reared individuals we interpret this as evidence of species-dependent environmental effects, perhaps associated with differences in habitat or light-environment preference. Where significant species differences are found for both comparisons we interpret this as evidence of heritable differences in brain development.

We collected published data for neuropil volumes of four other Lepidoptera; the Monarch butterfly (*D. plexippus*; Heinze and Reppert, 2012), the Zavaleta Glass wing (*Godyris zavaleta*; Montgomery and Ott, 2015), the Giant Sphinx moth (*Manduca sexta*; El Jundi et al., 2009b) and the Tobacco Budworm moth (*Heliothis virescens*; Kvello et al., 2009). Data were available for eight neuropils across all four species. We calculated the relative investment in each neuropil by comparing its volume to the total neuropil volume of either the whole brain (excluding the lamina, which was not measure in *Heliothis virescens*), or of only the midbrain. Relative size was measured by calculating the residuals from a phylogenetically-corrected least squares (PGLS) linear regression between each structure and the rest of the brain performed in BayesContinous in BayesTraits (freely available from www.evolution.rdg.ac.uk; Pagel, 1999). For this analysis, a phylogeny of the six species was created using data on two loci, *COI* and *EF1a* (GenBank Accession IDs, *COI*: EU069042.1, GU365908.1, JQ569251.1, JN798958.1, JQ539220.1, HM416492.1; *EF1a*: EU069147.1, DQ157894.1, U20135.1, KC893204.1, AY748017.1, AY748000.1). The data were aligned and concatenated using MUSCLE (Edgar, 2004), before constructing a maximum likelihood tree in MEGA v.5 (Tamura et al., 2011). Differences in brain architecture across species were visualised by multivariate Principal Component Analysis of these data, and visualized as biplots (Greenacre, 2010) in R package *ggbiplot* (V.Q. Vu, https://github.com/vqv/ggbiplot).

Finally, we extended our phylogenetic analysis across insects using a similar approach. We restricted this analysis to volumetric data collected with similar methodology (Rein et al., 2002; Brandt et al., 2005; Kurylas et al., 2008; Dreyer et al., 2010; Ott and Rogers, 2010; Wei et al., 2010) as it is not known how comparable data collected with alternative fixing, staining and imaging methods are. The phylogenetic relationship of these insects was taken from Trautwein et al. (2012).

RESULTS

General layout of the *Heliconius* brain

In general, the overall layout and morphology of the *Heliconius* brain (Fig. 1) is similar to that of other Lepidoptera (El Jundi et al., 2009; Kvello et al., 2009; Heinze and Reppert, 2012a; Montgomery and Ott, 2015). The midbrain forms a single medial mass, containing the supra-esophageal ganglion to which the sub-esophageal ganglion is fused. Synapsin immunostaining effectively labeled regions of synaptic neuropil, with minimal fluorescence in fiber tracts and cell bodies, permitting segmentation of six paired neuropils in the optic lobes, and eight paired and two unpaired neuropils in the midbrain. Together with the rest of the midbrain (rMid), which lacks distinct internal boundaries, we measured the volumes of these neuropils in 59 individuals across both species (Table 1). In the following we briefly describe the main anatomical features of the sensory neuropils, the central complex and the mushroom bodies in wild individuals. We then present the results of intra-specific comparisons between age groups, between wild and insectary-reared individuals, before moving to an analysis of inter-specific comparisons between *H. hecale* and *H. erato*, and across a wider taxonomic scale.

Sensory neuropil

As expected for a strongly visual, diurnal butterfly, the optic lobes (OL; Fig. 2A–H) account for a large proportion of total brain volume (approximately 64%). As is the case in both *D. plexippus* and *G. zavaleta* the lamina (La), two-layered medulla (Me) (Fig. 2E), accessory medulla (aMe), lobula (Lob) and lobula plate (Lop) are well defined and positioned in the OL as nested structures, running lateral to medial (Fig. 2A). The La has a distinct, brightly stained inner rim (iRim; Fig. 2E), a feature

common to all diurnal butterflies analyzed thus far (Heinze and Reppert, 2012; Montgomery and Ott, 2015). In common with *D. plexippus* we identify a thin strip of irregularly shaped neuropil running ventrally from the aME to the Me (Fig. 2G–H).

We also identify a sixth neuropil in the OL that we believe to be homologous to the optic glomerulus (OG; Fig. 2B,F) identified in *D. plexippus* (Heinze and Reppert, 2012), which is absent in other Lepidopteran brains described to date and was postulated to be Monarch-specific. As in *D. plexippus* this neuropil is a multi-lobed, irregularly shaped structure positioned to the medial margin of the Lob with which it appears to be connected. In *Heliconius* the OG is not as extended in the anterior margin as *D. plexippus* and is subsequently confined to the OL, without protrusion into the optic stalk or midbrain (Fig. 2A,B,F). The position of the OG in *Heliconius* is also similar to that of a much smaller neuropil observed in *G. zavaleta* (Montgomery and Ott, 2015). We suggest these structures may be homologous but differentially expanded.

The midbrain contains two further neuropils with primary functions in processing sensory information; the anterior optic tubercule (AOTu), a visual center, and the antennal lobe (AL), the primary olfactory neuropil. We can identify all four components of the AOTu previously described in *D. plexippus* and *G. zavaleta* butterflies (Heinze and Reppert, 2012; Montgomery and Ott, 2015); the small, closely clustered nodular unit (NU), strap (SP) and lower unit (LU), and the much larger upper unit (UU) (Fig. 2C). As in other butterflies, the UU is expanded compared with nocturnal moths (El Jundi et al., 2009; Kvello et al., 2009). The proportion of total neuropil comprised of the AOTu is, however, larger in *D. plexippus* (0.736%) than *Heliconius* (0.400% in *H. hecale* and 0.368% in *H. erato*).

The AL are innervated by the antennal nerves and comprise the central fibrous neuropil (CFN) around which small, round glomeruli are arranged (Figure 3A,B). In *Heliconius* the AL comprises 2% of the total brain neuropil volume, and contains approximately 68 glomeruli (estimated in one individual of each sex: *H. erato* ♂ = 69, ♀ = 68; *H. hecale* ♂ = 68, ♀ = 67). This is similar to estimates for other Lepidoptera, which generally range between 60 and 70 (Boeckh and Boeckh, 1979; Rospars, 1983; Berg et al., 2002; Huetteroth and Schachtner, 2005; Masante-Roca et al., 2005; Skiri et al., 2005; Kazawa et al., 2009; Heinze and Reppert, 2012; Carlsson et al., 2013; Montgomery and Ott, 2015), and the number of olfactory receptor genes (70) identified in the *H. melpomene* genome (Dasmahapatra et al., 2012). We observe no

expanded macro-glomeruli or obvious candidates for sexual dimorphic glomeruli suggesting an absence of any MGC-like structure in *Heliconius*. This is in keeping with all diurnal butterflies described to date (Rospars, 1983; Heinze and Reppert, 2012; Carlsson et al., 2013), with the exception of the more olfactorily orientated *G. zavaleta* in which the AL is 5% of total neuropil volume and a sexually dimorphic MGC is observed (Montgomery and Ott, 2015).

We took advantage of comparable datasets for *H. erato*, *H. hecale* and *G. zavaleta* to further investigate the significance of changes in AL size by testing whether changes in relative AL volume are due to an increased volume of glomeruli or CFN. The former would reflect heightened olfactory sensitivity, as larger glomeruli receive more projections from sensory neurons, while the latter may indicate changes in the number or complexity of local interneurons. We find evidence for a grade-shift in the allometric relationship between total glomerular volume and midbrain volume when *G. zavaleta* is compared to either *H. erato* (Wald $\chi^2 = 10.709$, $p = 0.001$) or *H. hecale* (Wald $\chi^2 = 9.139$, $p = 0.003$) (Fig. 3C, circles). We also identify a grade-shift between CFN volume and midbrain volume in *G. zavaleta* over *H. erato* (Wald $\chi2 = 30.282$, $p < 0.001$) and *H. hecale* (Wald $\chi^2 = 26.638$, $p < 0.001$) (Fig. 3C, triangles). Hence, AL expansion in *G. zavaleta* is due to changes in both CFN and glomerular volume. However, when comparing CFN and glomerular volume directly against one another we again find a significant grade-shift in *G. zavaleta* over *H. erato* (Wald $\chi^2 = 19.680$, $p < 0.001$) and over *H. hecale* (Wald $\chi^2 = 31.663$, $p < 0.001$) demonstrating greater CFN volume, relative to glomerular volume, in *G. zavaleta* (Fig. 3D). This suggests variation in Lepidopteran AL size may be largely explained by changes in the complexity of olfactory processing, which may in turn explain the consistency in glomerular number across species with contrasting diel patterns (see above).

Central complex

The central complex is a multimodal integration center linked to a range of functions from locomotor control to memory (Pfeiffer and Homberg, 2014). Within the limitations of the current analysis, the anatomy of the *Heliconius* central complex shows strong conservation with *D. plexippus* and *G. zavaleta* (Heinze and Reppert, 2012; Montgomery and Ott, 2015). The central body (CB) is positioned along the midline of the central brain and is formed of two neuropils, the upper (CBU) and lower (CBL) divisions, which are associated with small paired neuropils, the noduli

(No), located ventrally to the CB (Fig. 4A–D,G). Two further paired neuropils, the protocerebral bridge (PB; Fig. 4A,E) and posterior optic tubercles (POTu; Fig. 4A,F), are positioned towards the posterior margin of the brain.

Mushroom bodies

The most striking aspect of *Heliconius* brain morphology are the hugely expanded mushroom bodies, previously noted by Sivinski (1989). These neuropils span the depth of the brain along the anterior-posterior axis (Fig. 5A–K; Fig. 6A,A'). On the anterior side, the mushroom body lobes (MB-lo) lie above the AL. As in *D. plexippus* (Heinze and Reppert, 2012a) the distinct lobe structure observed in moths (El Jundi et al., 2009; Kvello et al., 2009) is lost, possibly due to extensive expansion. The only identifiable feature is a lobe curving round the medial margin, likely to be part of the vertical lobe (Fig. 5D,F). The MB-lo merges with a long cylindrical neuropil, the pedunculus (MB-pe) that extends to the posterior midbrain and is comprised of several twisted layers of neuropil. The boundary between the MB-lo and MB-pe is not distinct. The combined volume of the MBlo+pe accounts for 12.2% of total midbrain volume in *H. hecale* and 14.6% of total midbrain volume in *H. erato*, at least twice that reported for other Lepidoptera (Sjöholm et al., 2005; El Jundi et al., 2009; Kvello et al., 2009; Heinze and Reppert, 2012a; Montgomery and Ott, 2015). At the posterior end, the MB-pe splits into two roots that are encircled by the mushroom body calyx (MB-ca; Fig. 5A,H,K). A Y-tract runs parallel to the MB-pe from the posterior boundary of the MB-lo to the junction between the MB-pe and MB-ca. The Y-tract ventral loblets seen in other Lepidoptera (El Jundi et al., 2009; Kvello et al., 2009) are not distinct, presumably having merged with the MB-lo (Fig. 5A,J,N).

The MB-ca is a deeply cupped, un-fused, double-lobe structure (Fig. 5A,C). Two concentric zones can be identified (Fig. 5E), though the boundary is not distinct throughout the depth of the neuropil. The MB-ca comprises 20.7% and 23.9% of total midbrain volume in *H. hecale* and *H. erato* respectively, at least three times greater than reported in other Lepidoptera (Sjöholm et al., 2005; El Jundi et al., 2009; Kvello et al., 2009; Heinze and Reppert, 2012a; Montgomery and Ott, 2015). In some individuals the MB-ca is so large that it protrudes into the OL resulting in a distortion of shape caused by constriction around the optic stalk (Fig. 5H). We also observe some degree of pitting in the posterior surface of the MB-ca (Fig. 5I). This pitting is

related to radially arranged columnar domains that are apparent within the calycal neuropil (Fig. 5J,K,M)

Below the junction between MB-pe and MB-ca is a brightly stained globular neuropil with a poorly defined anterior margin (Fig. 5M). It is possible this is an accessory calyx, which has a sporadic phylogenetic distribution across Lepidoptera and other insects (Farris, 2005). However, accessory calyces are generally positioned closely to the MB-pe/MB-ca, as is observed in *D. plexippus* (Heinze and Reppert, 2012). This neuropil also lacks the 'spotty' appearance of the accessory calyx in *D. plexippus* (Heinze and Reppert, 2012). We therefore do not believe this is an accessory calyx. Similar 'satellite' neuropils that are near, but not directly linked to the mushroom bodies are observed in other insects, for example *Neuroptera* (Farris, 2005). One potentially interesting observation is that this neuropil lies in a position roughly equivalent to the anterior end of the OG in *D. plexippus* (Heinze and Reppert, 2012). Although generally unclear, in some individuals it is possible to follow a narrow, weakly stained fiber tract from the medial margin of the Lob/OG to this position, via an area of relatively intense staining in the optic stalk (Fig. 5L). It is possible this neuropil is functionally connected to the OG, and that OG expansion along the anterior margin in *D. plexippus* occurred along the path of this pre-existing connection, resulting in a single, elongated neuropil. In other insects the MB-pe also receives afferent innervation from regions of the protocerebrum other than the MB-ca (Schürmann, 1970; Li and Strausfeld, 1997, 1999). A pronounced fiber tract emanating from the AOTu UU clearly runs against the dorsal boundary of the MB-pe (Figure 5O), but whether or not there is a functional connection, that might suggest the integration of processed visual information with the MB-pe/lo, is unclear.

Brain:body allometry

The relationship between total neuropil and body mass is not significant at $p > 0.05$ for either wild *H. hecale* (log-log SMA regression, $p = 0.055$) or wild *H. erato* ($p = 0.863$). However, as expected body mass is more variable than either body length or wingspan (*H. hecale*, relative SD of body mass = 15.32%, body length = 10.43%, wingspan = 9.08%; *H. erato*, relative SD of body mass = 19.00%, body length = 5.98%, wingspan = 4.59%), most likely due to differences in feeding and reproductive state. When either body length or wingspan is used as the measure of body size a significant association is recovered both in *H. hecale* (body length $p = 0.020$,

wingspan $p = 0.019$) and in *H. erato* (body length $p = 0.011$, wingspan $p = 0.010$). We subsequently used body length to compare the relationships between total neuropil volume and body size between groups.

We identified a significant grade-shift, between the young and old groups of both *H. erato* and *H. hecale*, in the scaling relationship between total neuropil and body length (*H. hecale:* Wald $\chi^2 = 5.780$, $p = 0.016$; *H. erato:* Wald $\chi^2 = 10.124$, $p = 0.001$). However, there is no significant difference in body length for either species between old and young insectary-reared individuals (*H. hecale* $t_{18} = -0.918$, $p = 0.371$; *H. erato* $t_{17} = 0.581$, $p = 0.568$) suggesting the effect is primarily driven by an increase in neuropil volume. Indeed, there is a significant difference in total neuropil volume between the young and old insectary-reared age groups in *H. erato* ($t_{17} = 5.153$, $p < 0.001$, $r = 0.708$; Fig. 7A). This difference is observed for both total midbrain volume ($t_{17} = 4.192$, $p = 0.001$, $r = 0.713$) and total OL volume ($t_{17} = 5.076$, $p < 0.001$, $r = 0.776$; Fig. 7A). In *H. hecale* a significant difference between young and old individuals is only observed for midbrain volume ($t_{18} = 3.054$, $p = 0.007$, $r = 0.595$), but not OL volume ($t_{18} = 0.280$, $p = 0.783$) or total neuropil volume ($t_{18} = 1.082$, $p = 0.293$; Fig. 7D).

In *H. hecale*, the total neuropil is also 40% larger in wild caught individuals than in old insectary-reared individuals ($t_{17} = 2.553$, $p = 0.020$, $r = 0.526$) driven by a significant difference in midbrain volume ($t_{17} = 3.658$, $p = 0.002$, $r = 0.664$), but not OL volume ($t_{18} = 1.728$, $p = 0.101$; Fig. 7D). We also do not observe a similar difference in body length between wild and old insectary-reared individuals (*H. hecale* $t_{18} = 0.983$, $p = 0.436$). Although this does not result is a grade-shift between wild and old insectary-reared individuals for body length and total neuropil volume (Wald $\chi^2 = 2.058$, $p = 0.151$), we do observe a grade-shift when midbrain is analysed separately (Wald $\chi^2 = 4.725$, $p = 0.030$) No significant volume or size differences are found between wild and old insectary-reared individuals in *H. erato* (total neuropil: $t_{17} = -0.432$, $p = 0.671$; midbrain: $t_{17} = -0.732$, $p = 0.474$; OL: $t_{17} = -0.123$, $p = 0.904$; body length: $t_{17} = 1.009$, $p = 0.327$; Fig. 7A).

Post-eclosion growth in the volume of individual neuropil regions

Evidence of significant age-effects on volume was uncovered for many neuropil regions in both species, indicating an important role for post-eclosion brain

maturation. In *H. erato* volumetric differences between the age groups are widespread, with only the OG failing to show a significant expansion in old individuals (Table 2A). There is some evidence for age-related differences in the allometric scaling coefficients for aMe and PB, and for grade-shifts in OG and POTu, but these are weak relative to the strong major axis shifts observed for all segmented neuropils (Table 2A). The largest shifts are observed for the POTu (difference in fitted-axis (FA) mean = 0.604), aME (difference in FA mean 0.536), MB-ca (difference in FA mean = 0.496) and MB-lo+ped (difference in FA mean = 0.393; Fig. 6A-C).

In *H. hecale* old insectary-reared individuals have significantly larger absolute midbrain volumes (t_{18} = 3.054, p = 0.007, r = 0.584) but not OL volumes (t_{18} = 1.728, p = 0.101). However, not all segmented midbrain neuropil show the same expansion; the rMid, components of the mushroom body complex, central complex and AL are all significantly larger in old individuals, but the AOTu, POTu and all optic lobe neuropil are not (Table 2B). Neuropil expansion appears to occur in a co-ordinated manner, maintaining the allometric relationship between the segmented neuropil and rMid (Table 2B). The only exceptions are the La, Me and OG, which show significant grade-shifts resulting in a reduced volume of these neuropil relative to rMid volume in old individuals. All other segmented neuropil show major-axis shifts along a common slope towards higher values in old individuals (Table 2B). The largest shifts are observed for the MB-ca (difference in fitted-axis mean = 0.279) and MB-lo+ped (difference in fixed axis mean = 0.250; Fig. 6A'–C').

Experience-dependent plasticity in neuropil volume

The strong contribution of post-emergence growth to brain maturation in *Heliconius* provides a potential window during which the environment could influence the size of different neuropil. We compared wild and old insectary-reared individuals to test for the presence of such environment-dependent neural plasticity. A clear signature of environmentally induced volumetric differences is found in both species, but the pattern differs between them.

In *H. erato* wild individuals do not have significantly larger absolute neuropil volumes for any measured trait (Table 3A). However, several neuropils show evidence of differences in allometric scaling or grade-shifts between wild and old insectary-reared individuals. The neuropil affected by altered scaling coefficients (β)

include the MB-ca, the Lop, and the PB, all of which result shallower scaling realtionships with rMid volume in wild caught individuals (Table 3A; Figure 7B,C). The MB-lo+ped is the only neuropil to show an unambiguous grade-shift whilst maintaining a common slope, and also shows a major axis shift (difference in FA mean = 0.250; Fig. 6B).

In *H. hecale* wild individuals have significantly larger total midbrains (t_{18} = 3.658, p = 0.002). The only segmented neuropil to reflect this difference are the MB-ca and MB-lo+ped (Table 3B; Fig. 6A'-C'), while the rMid is also larger in wild individuals (t_{18} = 3.417, p = 0.003). For example, the average MB-ca volume of old insectary-reared individuals is only 68.3% of the average wild MB-ca volume, for the young insectary-reared individuals it is 49.3% (Figure 6A',C'). For MB-lo+pe these figures are 76.9% and 58.7% respectively (Figure 6A',B'). For comparison, in *H. erato* the average MB-ca volume of old insectary-reared individuals is 96.2% of the average wild MB-ca volume, for the young insectary-reared individuals it is 59.7% (Fig. 6A–C). For MB-lo+pe these figures are 96.9% and 63.9% respectively (Fig. 6A–C).

The only neuropil in the optic lobes to differ significantly volume in *H. hecale* is the Me. The allometric relationship between neuropil volumes and rMid differs for all neuropil either in the allometric scaling coefficient or the intercept, except for the mushroom body components and aMe.(Table 3A; Figure 7E,F). However, for aME this pattern is caused by a lack of allometric scaling in insectary-reared individuals (SMA p = 0.552). The mushroom bodies show evidence of a major axis shift along a common slope (difference in FA mean MB-ca = 0.355, MB-lo+ped = 0.299). Given all grade-shifts result in smaller neuropil volumes relative to rMid (Fig. 7E,F) volume we interpret this as indicating the rMid and mushroom bodies show coordinated environment-dependent increases in volume whilst other neuropil volumes remain largely constant, but with subsequently altered allometric relationships with rMid.

These results highlight potential differences in the maturation and plasticity of brain size and structure between *H. hecale* and *H. erato*. Most notably the rMid appears to have greater amounts of environment-dependent growth in *H. hecale* which results in altered scaling relationships with other neuropil. In *H. hecale* this is accompanied by coordinated expansion of the mushroom body components, which, in volumetric terms is less pronounced in *H. erato*. Instead, the mushroom bodies, along

with PB and LoP, are relatively larger in wild *H. erato* due to a grade-shift in the scaling relationship with rMid.

Divergence in brain composition between *H. hecale* and *H. erato*

H. hecale is significantly larger than *H. erato* for all body size measurements (wild caught: body mass $t_{17} = 7.262$, $p < 0.001$; body length $t_{17} = 5.442$, $p < 0.001$; wingspan $t_{17} = 6.071$, $p < 0.001$). *H. hecale* also have larger midbrain ($t_{17} = 2.713$, $p = 0.014$, $r = 0.539$) and OL volumes ($t_{17} = 2.866$, $p = 0.010$, $d = 1.351$). This difference does not, however, match the body size difference, resulting in a grade-shift in the allometric relationship between body length and total neuropil volume between the species (Wald $\chi^2 = 5.695$, $p = 0.017$; Fig. 7A). This is predominantly driven by a grade shift in OL:body allometry (Wald $\chi^2 = 8.257$, $p = 0.004$; Fig. 8B) rather than in midbrain:body allometry (Wald $\chi^2 = 3.805$, $p = 0.051$; Fig. 8C). Hence, *H. erato* have larger OL volumes relative to body size than *H. hecale*. The same pattern is observed in old insectary-reared individuals suggesting this is not an environmentally induced difference (midbrain: Wald $\chi^2 = 1.721$, $p = 0.189$; OL Wald $\chi^2 = 11.131$, $p < 0.001$).

Among segmented neuropils only the La and Me show significant absolute volumetric differences between wild-caught individuals of the two species, both being larger in *H. hecale* (Table 4A). Analyses of allometric relationships imply species differences in neuropil investment (Table 4A). La and Me show strong major-axis shifts and we identify evidence for grade-shifts between rMid and aMe, Lob, LoP and OG, as well as all segmented neuropil in the midbrain except the PB and POTu (Table 4A). In all of these cases the shift is towards larger relative volumes in *H. erato*, and may be partially driven by the differences in rMid volume which is significantly larger in *H. hecale* ($t_{17} = 3.582$, p = 0.002. $r = 0.656$). Only one neuropil, the AL, shows evidence for a difference in the allometric coefficient β between species. The AL scales with a significantly higher coefficient in *H. erato* ($\beta = 1.197$, 95% C.I. = 0.699–2.05) than *H. hecale* ($\beta = 0.470$, 95% C.I. = 0.313–0.705), indicating the ALs of *H. erato* show a greater proportional increase in size as rMid increases than in *H. hecale*.

Species differences between old insectary-reared individuals are notably less widespread (Table 4B). The La is the only neuropil with a significant absolute volumetric difference between species, and notably rMid volume is also not

significantly different (t_{17} = -1.391, p = 0.181). There is no evidence for species differences in scaling coefficients for AL, and grade-shifts are restricted to Lam, Me, and OG. However, the direction of the grade-shifts indicates *H. hecale* have relatively larger component volumes. The difference in results between wild and old insectary-reared individuals is most probably explained by species differences in environment-dependent changes in rMid volume. The expanded rMid volume in wild individuals masks the grade-shifts observed in La and Me in old insectary-reared individuals and, because other segmented neuropil do not show a similar expansion, lead to the wide-spread grade-shifts observed between wild caught *H. hecale* and *H. erato*. The effect is even sufficient to reverse the direction of grade-shift for CB and LoP. These results imply role for environmentally induced plasticity in contributing to species differences, but also indicate environment-independent differences exist.

Discrimant Function Analysis (DFA) of component volumes is able to distinguish wild individuals of the two species along one major axis, correctly assigning 100% of samples to the correct species (Fig. 8D). Wilks Lambda suggests group differences explain 90% of total variance between samples, although the formal statistical test for a group difference does not reach significance (χ^2 = 20.76, 14 degrees of freedom, p = 0.108). To test whether phenotypic differentiation between species is caused by both environmentally independent and dependent variation we performed an additional DFA using four data-groups: i) wild *H. erato*, ii) old insectary-reared *H. erato*, iii) wild *H. hecale*, iv) old insectary-reared *H. hecale*. This analysis reduced the variation along three axes (Table 5A,B; Fig. 8E,F) which assign 87.2% of individuals to the correct data-group. No individuals were assigned to the wrong species, incorrect assignment always occurred between wild and old groups of the same species.

We subsequently performed a MANOVA to test for whether DF1, DF2 and DF3 are associated with species and/or group (wild vs. old), and to test for significant species-group interactions (Table 6C). DF1 showed a significant association with both species and group, DF2 and DF3 were specifically associated with group. Only DF2 showed a significant species by group interaction. Visual inspection of Discrimant Function plots (Fig. 8E,F) suggests DF2 separates wild and old insectary-reared individuals more effectively in *H. hecale*.

Divergence in brain composition across Lepidoptera and other insects

Beyond *Heliconius* there is a clear signature of adaptive divergence in the composition of Lepidoptera brains. We combined the data collected for the present analysis with comparable volumetric data for eight neuropils from four other species (as collated in Montgomery and Ott, 2015, Table 3; Fig. 9A). After correcting for allometric scaling, using phylogenetically-corrected regressions against total neuropil volume, the six species can be separated along two principal components that together explain 90.7% of variance. PC1 is heavily loaded by sensory neuropil in the negative direction, and the MB-ca and MB-lo+ped in the positive direction (Table 6). PC2 is heavily loaded by the Me in the positive direction and the AL and CB in the negative direction. This separates the six species into three pairs, representing (i) *H. hecale* and *H. erato*; (ii) the other diurnal butterflies, *D. plexippus* and *G. zavaleta*); and (iii) the night-flying moths, *H. virescens* and *M. sexta* (Fig. 9B). When midbrain neuropil are analyzed separately, PC1, which explains 68.7% of variance, marks an axis dominated by the AL, CB and MB components. PC2, which explains an addition 23.3% variance, is strongly loaded by the AOTu (Fig. 9C). This leads to two clusters grouping (i) *H. hecale* and *H. erato*, which invest heavily in mushroom body neuropil, and (ii) the night-flying moths and *G. zavaleta*, which invest heavily in olfactory neuropil; leaving *D. plexippus* isolated by its large AOTu volume. Although this could be partially explained by the AOTu appearing small in *Heliconius* due to the expanded mushroom bodies, when the MB volume is removed from total midbrain, *D. plexippus* still has the largest residual AOTu size, suggesting this is a genuine signal of divergence. Whether the larger AOTu volume in *D. plexippus* is derived, or more typical for diurnal butterflies, is not known.

Finally, we consider the most notable adaptation in *Heliconius* brains, the increase in mushroom body volume, in a wider phylogenetic context. The combined volume of the calyx, pedunculus and lobes accounts for 13.7% of total brain neuropil volume in *H. erato*, and 11.9% in *H. hecale*. This is much larger than reported for any other Lepidoptera measured with similar methods (range 2.3-5.1%). Expressed as a percentage of the midbrain, to remove the effects of variation in the large OL, *H. erato* (38.5%) and *H. hecale* (32.9%) again exceed other Lepidoptera (4.8-13.5%) by 3–7 fold. These figures are also much larger than reported for *H. charithonia* (4.2% of total brain size) by Sivinski (1989), whose figures for other Lepidoptera are also much lower suggesting the difference is probably explained by variation in methodology. However, Sivinski reported the mushroom bodies of *H. charithonia* to

be approximately 4-times larger than those of the other butterflies measured, which is similar to the fold differences we observe here.

Comparisons beyond Lepidoptera are complicated by differences in the neuropil measured. For example, the total neuropil volume is not reported for the *Tribolium* (Dreyer et al., 2010), *Leucophaea* (Wei et al., 2010) or *Drosophila* (Rein et al., 2002) brains, which instead report individual neuropil volumes as a percentage of the sum of all segmented components. The most well matched comparisons are to *Apis mellifera* (Brandt et al., 2005) and *Schistocerca gregaria* (Kurylas et al., 2008) for which mushroom body volume and midbrain volume are reported (Fig. 9D). Even here, however, the data is not fully comparable, as the SOG is not fused with the midbrain in *S. gregaria*. In *A. mellifera* the mushroom bodies comprise 65.4% of the midbrain, (40.6% MB-ca, 24.8% MB-lo+ped) (Brandt et al., 2005), in gregarious-phase *S. gregaria* they comprise 15.1% (8.2% MB-ca including the accessory calyx, 6.3% MB-lo+ped) (Kurylas et al., 2008). Ott and Rogers (2010) report proportional calyx volumes in *S. gregaria* of 7.6% and 8.6% in solitarious-phase and gregarious-phase locusts, respectively (both figures include the accessory calyx), but did not measure the peduncle. In terms of raw volume our estimates (Table 1) *Heliconius* mushroom bodies are roughly equal in size to *A. mellifera*.

More general comparisons can be made expressing mushroom body size as a percentage of segmented neuropil (Me+Lobula system, CB, MB and AL) that were labeled across a wider range species (Dreyer et al., 2010). In this analyses *A. mellifera*, *T. castaneum* and *L. madera* all devote a larger proportion of total neuropil to the mushroom bodies than *Heliconius.* However, they also have substantially smaller optic lobes. If one instead examines the ratio of percentage mushroom body volume to the percentage of the two other midbrain neuropil (AL and CB), *Heliconius* have the largest ratios (*H. erato*: 6.4; *H. hecale*: 6.7) by some way, exceeding even *A. mellifera* (3.8). Similarly, the residuals from the highly significant ($p < 0.001$) PGLS regression (Fig. 9E) between percentage OL and percentage MB for *Heliconius* (*H. erato* +8.2; *H. hecale* +7.5) are only exceeded by *A. mellifera* (+11.9), which both far exceed the forth-largest residual (*S. gregaria* +2.2). A similar result is found comparing percentage MB to percentage AL+CB. This fairly crude analysis at least demonstrates that *Heliconius* rank highly across insects in terms of investment in mushroom body neuropil.

DISCUSION

We have described the layout and volume of the major neuropils in the brain of two species of *Heliconius* butterflies. We have further demonstrated patterns of variation across age groups of insectary-reared and wild individuals that are consistent with significant post-eclosion growth and experience-dependent plasticity in neuropil volume. Our analyses confirm previous reports of a substantial expansion in mushroom body size during the evolution of *Heliconius* butterflies (Sivinski, 1989). Indeed, our data suggest this previous work underestimated the proportional size of the *Heliconius* mushroom bodies. We further demonstrate levels of plasticity in mushroom body volume comparable to those found in foraging insects known for their capacity to learn spatial information (e.g. Withers et al., 1993, 2008; Gronenberg et al., 1996; Fahrbach et al., 1998, 2003; Maleszka et al., 2009; Jones et al., 2013). However, plasticity is not limited to the mushroom bodies, nor is the signal of adaptive divergence in neuropil structure. In the following, we discuss how and why *Heliconius* may have evolved such large mushroom bodies, what the convergent expansion of the mushroom body in independent insect lineages can tell us about their function and significance, and finally widen our scope to consider how the brains of different Lepidoptera are adapted to their different ecological niches.

Mushroom body expansion in Heliconius

As a percentage of total brain volume, or indeed as a raw volume, *Heliconius* have the largest mushroom body so far reported in Lepidoptera (Sivinski, 1989; Sjöholm et al., 2005; Rø et al., 2007; Kvello et al., 2009; Snell-Rood et al., 2009; Dreyer et al., 2010; Heinze and Reppert, 2012b; Montgomery and Ott, 2015). The expansion affects the calyx, pedunculus and lobes. The calyx has an expanded double-lobe, deeply cupped structure, superficially reminiscent of the mushroom body calyx of *A. mellifera* (Brandt et al., 2005), but structurally quite different from the calyx of *Danaus plexippus* which is composed of a series of concentric sub-structures that are not deeply cupped. As in *D. plexippus* (Heinze and Reppert, 2012) and to a lesser extent *Godyris zavaleta* (Montgomery and Ott, 2015), the lobe system is sufficiently expanded to merge individual lobes that are distinct in *Manduca sexta* and *Heliothis virescens* (Sjöholm et al., 2005; Rø et al., 2007; El Jundi et al., 2009; Kvello et al.,

2009). This precludes an accurate assessment of whether all lobes are equally expanded with the current data, which would be of interest given their relationship to different aspects of memory (Krashes et al., 2007; Guven-ozkan and Davis, 2014; Stopfer, 2014). It appears likely however that both the α'/β' and α/β lobes, which are responsible for consolidating long-term memory, and for the retrieval and expression of these memories (Guven-ozkan and Davis, 2014), contribute to the expansion.

Mushroom body expansion suggests the presence of selection for greater memory capacity during *Heliconius* evolution. The unique pollen-feeding behavior of adult *Heliconius*, and associated demands of foraging for spatially distributed resources, provides the most likely source of this selection pressure (Gilbert, 1975; Sivinski, 1989). Several studies have reported evidence of spatially and temporally faithful foraging patterns (Ehrlich and Gilbert, 1973; Gilbert, 1975, 1993; Mallet, 1986) comparable with the well described trap-lining behavior of foraging bees (Janzen, 1971; Heinrich, 1979). In hymenoptera, this behavior involves landmark based spatial memory (Cartwright and Collett, 1983; Dyer, 1991; Menzel et al., 2005). Mushroom bodies are implicated in spatial memory both through experimental manipulation (Mizunami et al., 1998) and comparative neuro-ecological studies (Farris and Schulmeister, 2011), although the role selection for spatial memory played in mushroom body expansion in Hymenoptera remains unproven for some authors (Menzel, 2014).

Comparisons across *Heliconius* and non-pollen feeding genera in the Heliconiini may provide a test of this hypothesis. Sivinski (1989) reported that two individuals of *Dione juno* and *Dryas iulia*, both non-pollen feeding allies to *Heliconius*, have mushroom bodies within the range of other Lepidoptera. This provides preliminary support that mushroom body expansion may have occurred co-incidentally with a single origin of pollen feeding at the base of *Heliconius*. However, several genera were not sampled, including the specious genus *Euides* which is most closely related to *Heliconius* (Beltrán et al., 2007; Kozak et al., 2015). As such, further sampling is required to confirm this conclusion. This work is underway. It is also conceivable alternative selection pressures may play a role, such as the degree of host-plant specialization (Brown, 1981) or the evolution of social roosting (Benson, 1972; Mallet, 1986). It is possible these factors are inter-related, as *Passiflora* may be incorporated into trap-lines between pollen plants (Gilbert, 1975, 1993), and the sedentary home-range behavior required for trap-lining may predispose *Heliconius* to

sociality (Mallet, 1986). Indeed, Farris and Schulmeister (2010) suggest sociality in hymenoptera is an exaptation, dependent on the co-option of a pre-existing elaboration of the mushroom bodies in response to the demands for spatial foraging in parasitic Euhymenopteran. Similar hypotheses have been proposed in vertebrates, for example, the initial expansion of the primate brain may have been driven by visual specialization (Barton, 1998). Social intelligence may therefore be viewed as an exaptation of this initial expansion that facilitated processing of a greater range and complexity of information (Barton and Dunbar, 1997).

It is certainly likely that pollen feeding at least plays a role in meeting the energetic costs of increased neural investment, even if it does not explain its origin. Increased investment in both the neural tissue required for learning-based foraging (Aiello et al., 1995; Laughlin et al., 1998; Snell-Rood et al., 2009) and the act of learning itself (Mery and Kawecki, 2004; Burger et al., 2008; Snell-Rood et al., 2009, 2011) will impose significant energetic costs, potentially resulting in trade-offs against other traits (Dukas, 1999; Burns et al., 2011; Snell-Rood et al., 2011; Snell-Rood, 2013). The fitness benefits of pollen-feeding lie in increased longevity without reproductive senescence (Dunlap-Pianka et al., 1977), facilitating a shift in the energetic costs of chemical defense to larvae as adults are no longer dependent on larval fat body stores (Cardoso and Gilbert, 2013), and amino acid transfer to eggs (O'Brien et al., 2003). These combined effects must outweigh the energetic costs incurred by greater neuropil investment.

Post-eclosion growth in mushroom body volume

Heliconius are not as robust to environmental perturbation, or as amenable as experimental subjects, as honeybees and ants. As a result our conditions are perhaps less controlled than comparable studies in these insects. Nevertheless, there is a clear effect of age on mushroom body size (Fig. 6). In both species, the mushroom bodies are significantly larger in aged individuals. These volume differences of 38.0% for the calyx and 34.0% for the lobe system in *H. erato,* and 27.9% for the calyx and 23.7% for the lobe system in *H. hecale* are comparable, if not greater than, the effects seen in Hymenoptera (e.g. c. 30% in *Camponotus floridanus* (Gronenberg et al., 1996); c. 20% in *Bombus impatiens* (Jones et al., 2013)).

Our comparisons between aged insectary-reared individuals and wild caught individuals also identify experience-dependent plasticity. This 'experience' in the

wild likely includes a greater range of movement as well as a greater complexity of foraging, and more variable environmental conditions and social interactions. In both species we see evidence for mushroom body plasticity, however it is notable that the pattern differs between species. In *H. hecale* a strong volumetric difference is found between old insectary-reared and wild caught individuals for both the calyx (32% difference) and lobes (24% difference). Again, this is a result of a major-axis shift in the unsegmented midbrain. This is not just an effect of increases in total brain size, as no other neuropil shows a similar increase resulting in widespread grade-shifts towards smaller relative size in wild caught individuals. This may suggest a coordinated pattern of growth between the mushroom bodies and unsegmented areas of the midbrain or alternatively independent plasticity in the two structures. In *H. erato* the effect of environmental plasticity is somewhat different. Although we find similar volumes in old insectary-reared individuals and wild caught individuals, both the mushroom body clayx and lobe system show allometric grade-shifts resulting in greater volumes relative to the unsegmented midbrain in wild individuals compared to insectary-reared individuals. It is also notable that this grade-shift is apparent because, in contrast to *H. hecale*, *H. erato* does not show a concomitant increase in midbrain volume in wild individuals.

It is currently unclear what causes this species difference. The difference may reflect changes in connectivity between the mushroom bodies and neuropil housed in the unsegmented midbrain, or perhaps experience-dependent plasticity in unrelated midbrain structures. Alternatively, the difference may be a sampling artifact. Although the ages of the insectary-reared individuals are not significantly different, we cannot rule out that the age structure of wild-caught individuals is biased. A further possibility is that *H. erato* and *H. hecale* respond differently to conditions in captivity, perhaps due to contrasting natural behavior in the wild. Nevertheless, our observation that *Heliconius* mushroom bodies show similar levels of post-eclosion growth to Hymenoptera, and a similar two-phase pattern of environmentally independent and dependent growth, provides further evidence of evolutionary convergence with *Heliconius*.

These large, volumetric changes in mushroom body size presumably have some significance on how the mushroom bodies are functioning. Some insight into the functional significance may be gained from investigating what is causing the increase in volume. Ongoing proliferation of Kenyon cells seems unlikely, if

neurogenesis is restricted to the larval and pupal stages, as it is in Hymenoptera (Masson, 1970; Fahrbach et al., 1995). Instead the increased volume may indicate changes in dendritic growth, as is suggested for mushroom body plasticity in Hymenoptera (Gronenberg et al., 1996; Farris et al., 2001). Farris et al. (2001) demonstrated age and experience dependent plasticity in dendrite branching. The former reflecting developmentally programmed growth of extrinsic neuron processes into the mushroom bodies, and the latter reflecting an expansion in the complexity of Kenyon cell processes. The resulting changes in dendritic fields may indicate altered neural connectivity.

Finally, although the mushroom bodies show the strongest and most consistent effects, it is also striking that plasticity, and in particularly age related growth, is not restricted to the mushroom bodes. This has been observed in other insects (Kühn-Bühlmann and Wehner, 2006; Snell-Rood et al., 2009; Ott and Rogers, 2010; Smith et al., 2010; Heinze and Florman, 2013; Jones et al., 2013). As in previous examples significant age-dependent effects in *Heliconius* appear to play a role in the development of sensory neuropil involved in the processing of both visual and olfactory information. This may not be unexpected as sensory neuropil do not merely relay information on to the central brain, but also process information *in situ* (Muscedere et al., 2014). Both the medulla and lobula system are implicated in processing different types of visual information (Paulk et al., 2009a; b). Similarly, odor learning may be due to plasticity in the antennal lobes themselves rather than, or as well as, higher order structures (Hammer and Menzel, 1998; Rath et al., 2011). We also find evidence of plasticity in the central complex. In Lepidoptera, the plasticity in central body has been demonstrated in response to experience with novel host plants (Snell-Rood et al., 2009), whilst the protocerebral bridge increases in volume following migratory experience in *D. plexippus* (Heinze et al., 2013). Our results suggest *Heliconius* may provide a useful system within which to explore the behavioral relevance of plasticity in the mushroom bodies, and other structures.

Convergent expansion of mushroom bodies: similarities and differences

Extensive mushroom body expansion is now reported in lineages of four insect orders; Dictyoptera, herbivorous Scarabaeidae, Hymenoptera, and *Heliconius* (Farris, 2013). We see three ecological traits that are shared by at least two of these lineages: dietary adaptations, central place foraging, and sociality. In scarab beetles mushroom

body expansion is associated with a shift from coprophagy to a generalist phytophagus diet, possibly in response to increased behavioral flexibility in the context of foraging (Farris and Roberts, 2005). It is conceivable a similar selection pressure may apply to cockroaches. In contrast, the initial increase in mushroom body size coincides with the origin of a specialist foraging behavior in Hymenoptera, parasitoidism (Farris and Schulmeister, 2011). As discussed above, the expansion of the *Heliconius* mushroom bodies may also be related to a specialist foraging behavior. In these cases, central place foraging may have facilitated the origin of more social behavior (Mallet, 1986; Farris and Schulmeister, 2011), which may have secondarily led to further increases in mushroom body volume (Dujardin, 1859; Withers et al., 1993; Gronenberg et al., 1996; Ehmer and Ron, 1999). The common theme of these hypotheses is that mushroom body expansion evolves in response to the need for parsing a greater complexity of environmental information, facilitating the emergence of new behaviors (Chittka and Niven, 2009).

Two anatomical traits associated with mushroom body expansion provide support for this hypothesis: increased complexity of sensory input into the mushroom bodies, and subdivision of the mushroom body calyx. In addition to olfactory inputs, the mushroom body calyx receives direct input from the optic lobes in Hymenoptera and phytophagus Scarab beetles (Gronenberg, 2001; Farris and Roberts, 2005; Farris and Schulmeister, 2011). This increase in functional inputs is reflected in the subdivision of the calyx into the lip, which processes olfactory information, and the collar and basal ring, which process visual information (Gronenberg and Hölldobler, 1999). This suggests mushroom body expansion may be partly caused by the acquisition of new functions (Farris, 2013).

It is not known whether *Heliconius* receive visual input into the mushroom bodies. However, this has been demonstrated in species of both butterflies (Snell-Rood et al., 2009) and moths (Sjöholm et al., 2005), and some anatomical features of the *Heliconius* brain suggest the possibility that this does occur. It is notable, however, that *Heliconius* lack clear subdivision of the calyx as seen in Hymenoptera. In contrast, Heinze and Reppert (2012) described clear structural subdivision, or zonation, that they postulated may be analogous to the *A. mellifera* lip, collar and basal ring. We do not interpret the lack of clear zonation in *Heliconius* as evidence that there is no functional sub-division, as *Spodptera littoralis* displays localization of visual processing in the mushroom body calyx that is not apparent without labeling

individual neurons. Given the implied role for visual landmark learning in *Heliconius* foraging behavior (Jones, 1930; Gilbert, 1972, 1975; Mallet, 1986), it seems probable that there has been some integration of visual information processing with the mushroom bodies.

In other species the mushroom body also receives input relaying gustatory and mechanosensory information (Schildberger, 1983; Homberg, 1984; Li and Strausfeld, 1999; Farris, 2008). These may also be of relevance in *Heliconius* given the importance of gustatory and mechanosensory reception in host-plant identification (Schoonhoven, 1968; Renwick and Chew, 1994; Briscoe et al., 2013) and pollen loading (Krenn and Penz, 1998; Penz and Krenn, 2000), although it should be noted that there is currently no evidence these behaviors are learnt (Kerpel and Moreira, 2005; Salcedo, 2011; Silva et al., 2014).

Ecological adaptations in Lepidopteran brain composition

The mushroom body is not the only neuropil to display an adaptive signature of divergence. Our interspecific analysis across Lepidoptera strongly suggest a mosaic pattern of brain evolution (Barton and Harvey, 2000) in response to a species' specific ecological needs (Barton et al., 1995; Huber et al., 1997; Gronenberg and Hölldobler, 1999b; Montgomery and Ott, 2015). This pattern is particularly noticeable in the sensory neuropil (Fig. 9B). The relative volume of the visual neuropil closely reflects diel activity patters, whilst the size of the antennal lobe also appears to be strongly associated with activity pattern or a low-light diurnal niche. This is illustrated in a PCA of midbrain neuropil (Fig. 9C) which clusters the olfactorily driven butterfly *G. zavaletta* with night-flying moths (Montgomery and Ott, 2015). As expected, *Heliconius* are distinguished by their enlarged mushroom bodies, whilst *D. plexippus* is isolated along an axis of variation heavily loaded by the AOTu. This may reflect dependence on visual information typical of diurnal butterflies; however, removal of the mushroom bodies from the analysis does not explain this difference. It is possible therefore that AOTu expansion is particularly prominent in *D. plexippus* as suggested by Heinze and Reppert (2012). The AOTu plays a key role in relaying segregated visual pathways (Pfeiffer et al., 2005; Heinze and Reppert, 2011; Mota et al., 2011; Pfeiffer and Kinoshita, 2012), suggesting a plausible link between AOTu expansion and migratory behavior (Heinze and Reppert, 2012a; Heinze et al., 2013).

These macroevolutionary patterns of divergence between genera are mirrored to some extent in comparisons between *H. erato* and *H. hecale*. In Panama, *H. hecale* and *H. erato* differ in host-plant use (Merrill et al., 2013), and *H. hecale* are biased towards collecting large grained pollen whereas *H. erato* collect pollen from plant species that produce smaller grains (Estrada and Jiggins, 2002). Although this may reflect foraging differences, it is likely that the difference is largely driven by competitive exclusion of *H. erato* from a generally preferred pollen source (Estrada and Jiggins, 2002) as there is no difference in the efficiency of handling different pollen sizes in captivity (Penz and Krenn, 2000), or evidence that *H. erato* preferentially collect small pollen grains in other wild populations (Boggs et al., 1981; Cardoso, 2001). These data suggest *H. erato* and *H. hecale* may be using their environment differently, and therefore be exposed to contrasting conditions and selection pressures.

Focusing on wild caught individuals, where variation in neuropil volume may be most ecologically relevant, *H. hecale* have a significantly larger total brain size. This is largely due to the optic lobes, and undefined regions of the midbrain. At the level of specific neuropil only the lamina and medulla differ significantly between species. However, interpreting allometric grade-shifts between species is complicated by significant differences in unsegmented midbrain volume, which is used as the independent variable throughout. In old insectary-reared individuals the significant difference in lamina volume persists, suggesting this may be a non-plastic species difference, whilst the effects on midbrain volume may be environment dependent. This supports recent data showing divergence in corneal facet number and diameter which suggests visual adaptations in different micro-habitats may play a role in *Heliconius* diversification (Seymoure et al., in review).

The behavioral relevance of divergence and plasticity in unsegmented areas of the midbrain, which lack clear boundaries, is less obvious. Given its role in controlling the mandibles, proboscis and mouth parts (Rehder, 1989; Bowdan and Wyse, 2000), all of which are involved in pollen loading (Krenn and Penz, 1998; Penz and Krenn, 2000), it is possible the effect is largely driven by variation in the sub-esophageal ganglion caused by species differences in pollen handling in the wild. The development of phenotypic markers that permit consistent segmentation of different areas of the midbrain across species (e.g. Heinze and Reppert, 2012) in future studies will permit a test of this hypothesis.

Interspecific differences between *H. erato* and *H. hecale* in brain component volumes are sufficient to correctly group individuals by species in a discriminant function analysis. Further analysis of species and group (wild vs. old insectary-reared) suggest both environment independent and dependent variation contributes to these species differences. The potential role of phenotypic plasticity in facilitating ecological diversification by bridging fitness valleys is attracting renewed and growing interest (Pfennig et al., 2010; Snell-Rood, 2013). The numerous closely related sister-species of *Heliconius* that exist along environmental gradients (Jiggins et al., 1996; Jiggins and Mallet, 2000; Estrada and Jiggins, 2002; Arias et al., 2008) may provide an opportunity to test the importance of neural phenotypic plasticity in facilitating ecological shifts during speciation.

Conclusions and future prospects

We have described the layout and size of the major neuropil in two species of *Heliconius* butterflies. This has confirmed a previous report that this genus has dramatically expanded mushroom bodies (Sivinski, 1989). Moreover our estimates of the percentage of the brain occupied by the mushroom bodies suggest the initial values underestimated the size of the mushroom body. Indeed, in some comparisons, *Heliconius* rank among the top insect species in terms of investment in mushroom body neuropil. Through comparisons across different age groups, and between wild and insectary-reared individuals, we further demonstrate levels of plasticity comparable to hymenoptera, extensively studied models of mushroom body expansion and plasticity. Our interspecific analysis reveals patterns of divergence in brain composition between genera, and within *Heliconius*, that suggest a close correspondence to ecological variables. This analysis lays the groundwork for comparative and experimental analyses that will seek to dissect the costs, benefits, behavioral relevance and proximate basis of differential expansion in key neuropil.

Other acknowledgments

The authors are grateful to Adriana Tapia, Moises Abanto, William Wcislo, Owen McMillan, Chris Jiggins, and the Smithsonian Tropical Research Institute for assistance, advice, and the use of the *Heliconius* insectaries at Gamboa, Panama, and the Ministerio del Ambiente for permission to collect butterflies in Panama. We also

thank Judith Mank's research group at UCL for helpful advice and feedback, and the UCL Imaging Facility for help with confocal microscopy.

Conflict of interest statement

The authors declare no conflict of interest.

Role of authors

All authors read and approved the final manuscript. Study conception: SHM. Study design and preliminary experiments: SHM, RMM, SRO. Fieldwork and insectary rearing: SHM, RMM. Acquisition of data, analysis, interpretation and initial manuscript draft: SHM. Final interpretation and drafting: SHM, RMM, SRO.

Literature cited

Aiello LC, Wheeler P. 1995. The expensive-tissue hypothesis: the brain and the digestive system in human and primate evolution. Curr Anthropol 199–221.

Arias CF, Muñoz AG, Jiggins CD, Mavárez J, Bermingham E, Linares M. 2008. A hybrid zone provides evidence for incipient ecological speciation in Heliconius butterflies. Mol Ecol 17:4699–712.

Barton RA, Harvey PH. 2000. Mosaic evolution of brain structure in mammals. Nature 405:1055–1058.

Barton RA. 1998. Visual specialization and brain evolution in primates. Proc Biol Sci 265:1933–1937.

Barton RA, Dunbar RI. 1997. Evolution of the social brain. In: Whiten A, Byrne RW, editors. Machiavellian intelligence II: Extensions and evaluations. Cambridge University Press. p 240.

Barton RA, Purvis A, Harvey PH. 1995. Evolutionary radiation of visual and olfactory brain systems in primates, bats and insectivores. Philos Trans R Soc Lond B Biol Sci 348:381–92.

Beltrán M, Jiggins CD, Brower AVZ, Bermingham E, Mallet J. 2007. Do pollen feeding , pupal-mating and larval gregariousness have a single origin in *Heliconius* butterflies? Inferences from multilocus DNA sequence data. J Linn Soc 92:221–239.

Benson WW. 1972. Natural selection for Miillerian mimicry in *Heliconius erato* in Costa Rica. Science (80) 176:936–939.

Berg BG, Galizia CG, Brandt R, Mustaparta H. 2002. Digital atlases of the antennal lobe in two species of tobacco budworm moths, the Oriental *Helicoverpa assulta* (male) and the American *Heliothis virescens* (male and female). J Comp Neurol 446:123–134. A

Boeckh J, Boeckh V. 1979. Threshold and odor specificity of pheromone-sensitive neurons in the deutocerebrum of *Antheraea pernyi* and *A. polyphemus* (Saturnidae). J Comp Physiol A 132:235–242.

Boggs CL, Smiley JT, Gilbert LE. 1981. Patterns of pollen exploitation by *Heliconius* butterflies. Oecologia 48:284–289.

Bowdan E, Wyse GA. 2000. Temporally patterned activity recorded from mandibular nerves of the isolated subesophageal ganglion of *Manduca*. J Insect Physiol 46:709–719.

Brandt R, Rohlfing T, Rybak J, Krofczik S, Maye A, Westerhoff M, Hege H-C, Menzel R. 2005. Three-dimensional average-shape atlas of the honeybee brain and its applications. J Comp Neurol 492:1–19.

Briscoe AD, Macias-Muñoz A, Kozak KM, Walters JR, Yuan F, Jamie GA, Martin SH, Dasmahapatra KK, Ferguson LC, Mallet J, Jacquin-Joly E, Jiggins CD. 2013. Female behaviour drives expression and evolution of gustatory receptors in butterflies. PLoS Genet 9:e1003620.

Brown KS. 1981. The biology of *Heliconius*. Annu Rev Entomol 26:427–457.

Burger JMS, Kolss M, Pont J, Kawecki TJ. 2008. Learning ability and longevity: A symmetrical evolutionary trade-off in *Drosophila*. Evolution 62:1294–1304.

Burish MJ, Kueh HY, Wang SSH. 2004. Brain architecture and social complexity in modern and ancient birds. Brain Behav Evol 63:107–124.

Burns JG, Foucaud J, Mery F. 2011. Costs of memory: lessons from “mini” brains. Proc Biol Sci 278:923–929.

Capaldi EA, Robinson GE, Fahrback SE. 1999. Neuroethology of spatial learning: the birds and the bees. Annu Rev Psychol 50:651–682.

Cardoso MZ, Gilbert LE. 2013. Pollen feeding, resource allocation and the evolution of chemical defence in passion vine butterflies. J Evol Biol 26:1254–60.

Cardoso MZ. 2001. Patterns of pollen collection and flower visitation by *Heliconius* butterflies in southeastern Mexico. J Trop Ecol 17:763–768.

Carlsson MA, Schäpers A, Nässel DR, Janz N. 2013. Organization of the olfactory system of Nymphalidae butterflies. Chem Senses 38:355–67.

Cartwright BA, Collett TS. 1983. Landmark learning in bees - Experiments and models. J Comp Physiol A 151:521–543.

Chittka L, Niven J. 2009. Are Bigger Brains Better? Curr Biol19:R995–R1008.

Clayton NS, Krebs JR. 1995. Memory in food-storing birds: From behaviour to brain. Curr Opin Neurobiol 5:149–154.

Cohen J. 1988. Statistical power analysis for the behavioral sciences. 2nd ed. Hillsdale, NJ.: Lawrence Earlbaum Associates.

Dasmahapatra KK, Walters JR, Briscoe AD, Davey JW, Whibley A, Nadeau NJ, Zimin A V., Hughes DST, Ferguson LC, Martin SH, Salazar C, Lewis JJ, Adler S, Ahn S-J, Baker DA, Baxter SW, Chamberlain NL, Chauhan R, Counterman BA, Dalmay T, Gilbert LE, Gordon K, Heckel DG, Hines HM, Hoff KJ, Holland PWH, Jacquin-Joly E, Jiggins FM, Jones RT, Kapan DD, Kersey P, Lamas G, Lawson D, Mapleson D, Maroja LS, Martin A, Moxon S, Palmer WJ, Papa R, Papanicolaou A, Pauchet Y, Ray DA, Rosser N, Salzberg SL, Supple MA, Surridge A, Tenger-Trolander A, Vogel H, Wilkinson PA, Wilson D, Yorke JA, Yuan F, Balmuth AL, Eland C, Gharbi K, Thomson M, Gibbs RA, Han Y, Jayaseelan JC, Kovar C, Mathew T, Muzny DM, Ongeri F, Pu L-L, Qu J, Thornton RL, Worley KC, Wu Y-Q, Linares M, Blaxter ML, Ffrench-Constant RH, Joron M, Kronforst MR, Mullen SP, Reed RD, Scherer SE, Richards S, Mallet J, Owen McMillan W, Jiggins CD. 2012. Butterfly genome reveals promiscuous exchange of mimicry adaptations among species. Nature 487:94–8.

Dreyer D, Vitt H, Dippel S, Goetz B, El Jundi B, Kollmann M, Huetteroth W, Schachtner J. 2010. 3D standard brain of the Red Flour Beetle *Tribolium castaneum*: A tool to study metamorphic development and adult plasticity. Front Syst Neurosci 4:3.

Dujardin F. 1859. Mémoire sur le système nerveux des insectes. Ann Des Sci Nat comprenant la Zool 14:195–206.

Dukas R. 1999. Costs of memory: ideas and predictions. J Theor Biol 197:41–50.

Dunlap-Pianka H, Boggs CL, Gilbert LE. 1977. Ovarian dynamics in heliconiine butterflies: programmed senescence versus eternal youth. Science (80) 197:487–490.

Durst C, Eichmüller S, Menzel R. 1994. Development and experience lead to increased volume of subcompartments of the honeybee mushroom body. Behav Neural Biol 62:259–263.

Dyer F. 1991. Bees acquire route-based memories but not cognitive maps in a familiar landscape. Anim Behav 41:239–246.

Edgar RC. 2004. MUSCLE: multiple sequence alignment with high accuracy and high throughput. Nucleic Acids Res 32:1792–7.

Ehmer B, Ron H. 1999. Mushroom bodies of vespid wasps. J Comp Neurol 416:93–100.

Ehrlich PR, Gilbert LE. 1973. Population structure and dynamics of the Tropical butterfly *Heliconius ethilla*. Biotropica 5:69–82.

Estrada C, Jiggins CD. 2002. Patterns of pollen feeding and habitat preference among Heliconius species. Ecol Entomol 27:448–456.

Fahrbach SE, Farris SM, Sullivan JP, Robinson GE. 2003. Limits on volume changes in the mushroom bodies of the honey bee brain. J Neurobiol 57:141–151.

Fahrbach SE, Giray T, Robinson GE. 1995. Volume changes in the mushroom bodies of adult honey bee queens. Neurobiol Learn Mem 63:181–191.

Fahrbach SE, Moore D, Capaldi EA, Farris SM, Robinson GE. 1998. Experience-expectant plasticity in the mushroom bodies of the honeybee. Learn Mem 5:115–123.

Farris SM, Roberts NS. 2005. Coevolution of generalist feeding ecologies and gyrencephalic mushroom bodies in insects. Proc Natl Acad Sci U S A 102:17394–17399.

Farris SM, Robinson GE, Fahrbach SE. 2001. Experience- and age-related outgrowth of intrinsic neurons in the mushroom bodies of the adult worker honeybee. J Neurosci 21:6395–6404.

Farris SM, Schulmeister S. 2011. Parasitoidism, not sociality, is associated with the evolution of elaborate mushroom bodies in the brains of hymenopteran insects. Proc Biol Sci 278:940–951.

Farris SM. 2005. Evolution of insect mushroom bodies: old clues, new insights. Arthropod Struct Dev 34:211–234.

Farris SM. 2008. Tritocerebral tract input to the insect mushroom bodies. Arthropod Struct Dev 37:492–503.

Farris SM. 2013. Evolution of complex higher brain centers and behaviors: behavioral correlates of mushroom body elaboration in insects. Brain Behav Evol 82:9–18.

Finkbeiner SD. 2014. Communal roosting in heliconius butterflies (Nymphalidae): roost recruitment, establishment, fidelity, and resource use trends based on age and sex. J Lepid Soc 68:10–16.

Finlay B, Darlington R. 1995. Linked regularities in the development and evolution of mammalian brains. Science (80) 268:1578–1584.

Garamszegi LZ, Eens M. 2004. The evolution of hippocampus volume and brain size in relation to food hoarding in birds. Ecol Lett 7:1216–1224.

Gilbert LE. 1972. Pollen feeding and reproductive biology of *Heliconius* butterflies. Proc Natl Acad Sci USA 69:1403–1407.

Gilbert LE. 1975. Ecological consequences of a coevolved mutualism between butterflies and plants. In: Gilbert LE, Raven P, editors. Coevolution of animals and plants. p 210–240.

Gilbert LE. 1993. An evolutionary food web and its relationship to Neotropical biodiversity. In: W Barthlott, CM Naumann, K Schmidt-Loske, KL Schuchmann, editors. Animal-plant interactions in Tropical environments. Zoologisches Forschungsinstitut und Museum Alexander Koenig, Bonn, Germany. p 17–28.

Giurfa M, Menzel R. 2001. Cognitive architecture of a mini-brain. Adapt Learn An Interdiscip Debate 5:22 – 48.

Gonda A, Herczeg G, Merilä J. 2009a. Adaptive brain size divergence in nine-spined sticklebacks (*Pungitius pungitius*)? J Evol Biol 22:1721–1726.

Gonda A, Herczeg G, Merilä J. 2009b. Habitat-dependent and -independent plastic responses to social environment in the nine-spined stickleback (*Pungitius pungitius*) brain. Proc Biol Sci 276:2085–2092.

Gonda A, Herczeg G, Merilä J. 2013. Evolutionary ecology of intraspecific brain size variation: A review. Ecol Evol 3:2751–2764.

Greenacre MJ. 2010. Biplots in practice. Fundacion BBVA.

Gronenberg W, Heeren S, Hölldobler B. 1996. Age-dependent and task-related morphological changes in the brain and the mushroom bodies of the ant *Camponotus floridanus*. J Exp Biol 199:2011–9.

Gronenberg W, Hölldobler B. 1999. Morphologic representation of visual and antennal information in the ant brain. J Comp Neurol 412:229–40.

Gronenberg W. 2001. Subdivisions of hymenopteran mushroom body calyces by their afferent supply. J Comp Neurol 435:474–489.

Guven-ozkan T, Davis RL. 2014. Functional neuroanatomy of *Drosophila* olfactory memory formation. :519–526.

Hammer M, Menzel R. 1998. Multiple sites of associative odor learning as revealed by local brain microinjections of octopamine in honeybees. Learn Mem 5:146–156.

Heinrich B. 1979. Resource heterogeneity and patterns of movement in foraging bumblebees. Oecologia 40:235–245.

Heinze S, Florman J, Asokaraj S, El Jundi B, Reppert SM. 2013. Anatomical basis of sun compass navigation II: the neuronal composition of the central complex of the monarch butterfly. J Comp Neurol 521:267–98.

Heinze S, Reppert SM. 2011. Sun compass integration of skylight cues in migratory monarch butterflies. Neuron 69:345–358.

Heinze S, Reppert SM. 2012. Anatomical basis of sun compass navigation I: the general layout of the monarch butterfly brain. J Comp Neurol 520:1599–628.

Hofbauer A, Ebel T, Waltenspiel B, Oswald P, Chen Y, Halder P, Biskup S, Lewandrowski U, Winkler C, Sickmann A, Buchner S, Buchner E. 2009. The Wuerzburg hybridoma library against *Drosophila* brain. J Neurogenet 23:78–91.

Homberg U. 1984. Processing of antennal information in extrinsic mushroom body neurons of the bee brain. J Comp Physiol A Neuroethol Sens Neural Behav Physiol:825–836.

Huber R, van Staaden MJ, S K Les, Liem KF. 1997. Microhabitat use, trophic patterns, and the evolution of brain structure in African Cichlids. Brain Behav Evol 50:167–182.

Huetteroth W, Schachtner J. 2005. Standard three-dimensional glomeruli of the *Manduca sexta* antennal lobe: a tool to study both developmental and adult neuronal plasticity. Cell Tissue Res 319:513–24.

Janzen ADH. 1971. Euglossine bees as long-distance pollinators of tropical plants. Science (80) 171:203–205.

Jiggins C, Mallet J. 2000. Bimodal hybrid zones and speciation. Trends Ecol Evol 15:250–255.

Jiggins CD, Macmillan WO, Neukirchen W a. LT, Mallet J. 1996. What can hybrid zones tell us about speciation? The case of *Heliconius erato* and *H. himera* (Lepidoptera: Nymphalidae). Biol J Linn Soc 59:221–242.

Jiggins CD. 2008. Ecological speciation in mimetic butterflies. Bioscience 58:541.

Jones BM, Leonard AS, Papaj DR, Gronenberg W. 2013. Plasticity of the worker bumblebee brain in relation to age and rearing environment. Brain Behav Evol 82:250–261.

Jones F. 1930. The sleeping heliconias of Florida. Nat Hist 30:635–644.

El Jundi B, Huetteroth W, Kurylas AE, Schachtner J. 2009. Anisometric brain dimorphism revisited: Implementation of a volumetric 3D standard brain in *Manduca sexta*. J Comp Neurol 517:210–25.

Kazawa T, Namiki S, Fukushima R, Terada M, Soo K, Kanzaki R. 2009. Constancy and variability of glomerular organization in the antennal lobe of the silkmoth. Cell Tissue Res 336:119–36.

Kerpel SM, Moreira GRP. 2005. Absence of learning and local specialization on host plant selection by *Heliconius erato*. J Insect Behav 18:433–452.

Klagges BR, Heimbeck G, Godenschwege T a, Hofbauer a, Pflugfelder GO, Reifegerste R, Reisch D, Schaupp M, Buchner S, Buchner E. 1996. Invertebrate synapsins: a single gene codes for several isoforms in *Drosophila*. J Neurosci 16:3154–65.

Kozak KM, Wahlberg N, Dasmahapatra KK, Mallet J, Jiggins CD. 2015. Multilocus species trees show the recent adaptive radiation of the mimetic *Heliconius* butterlies. Syst Biol. *in press.*

Krashes MJ, Keene AC, Leung B, Armstrong JD, Waddell S. 2007. Sequential use of mushroom body neuron subsets during *Drosophila* odor memory processing. Neuron 53:103–115.

Krenn HW, Penz CM. 1998. Mouthparts of *Heliconius* butterflies (Lepidoptera : Nymphalidae): A search for anatomical adaptations to pollen-feeding behavior. Int J Insect Morphol Embryol 27:301–309.

Kühn-Bühlmann S, Wehner R. 2006. Age-dependent and task-related volume changes in the mushroom bodies of visually guided desert ants, *Cataglyphis bicolor*. J Neurobiol 66:511–521.

Kurylas AE, Rohlfing T, Krofczik S, Jenett A, Homberg U. 2008. Standardized atlas of the brain of the desert locust, *Schistocerca gregaria*. Cell Tissue Res 333:125–45.

Kvello P, Løfaldli BB, Rybak J, Menzel R, Mustaparta H. 2009. Digital, three-dimensional average shaped atlas of the *Heliothis virescens* brain with integrated gustatory and olfactory neurons. Front Syst Neurosci 3:14.

Laughlin SB, de Ruyter van Steveninck RR, Anderson JC. 1998. The metabolic cost of neural information. Nat Neurosci 1:36–41.

Li Y, Strausfeld NJ. 1997. Morphology and sensory modality of mushroom body extrinsic neurons in the brain of the cockroach, *Periplaneta americana*. J Comp Neurol 387:631–650.

Li Y, Strausfeld NJ. 1999. Multimodal efferent and recurrent neurons in the medial lobes of cockroach mushroom bodies. J Comp Neurol 409:647–63.

Lihoreau M, Latty T, Chittka L. 2012. An exploration of the social brain hypothesis in insects. Front Physiol 3:1–7.

Maleszka J, Barron AB, Helliwell PG, Maleszka R. 2009. Effect of age, behaviour and social environment on honey bee brain plasticity. J Comp Physiol A Neuroethol Sensory, Neural, Behav Physiol 195:733–740.

Mallet J. 1980. A laboratory study of gregarious roosting in the butterfly *Heliconius melpomene*. MSc Thesis. UCL Eprints no. 1301849 (http://discovery.ucl.ac.uk/1301849)

Mallet J. 1986. Gregarious roosting and home range in *Heliconius* butterflies. Natl Geogr Res. 2:198-215

Mallet J. 1993. Speciation, raciation, and color pattern evolution in *Heliconius* butterflies: evidence from hybrid zones. In: Harrison RG, editor. Hybrid zones and the evolutionary process. Oxford University Press. p 226–260.

Masante-Roca I, Gadenne C, Anton S. 2005. Three-dimensional antennal lobe atlas of male and female moths, *Lobesia botrana* (Lepidoptera: Tortricidae) and glomerular representation of plant volatiles in females. J Exp Biol 208:1147–59.

Masson C. 1970. Mise en évidence, au cours de l'ontogénèse d'une fourmi primities (*Mesoponera caffraria* F.Smith), d'une prolifération tardive au niveau des cellules golbuleuses (Globuli-cells) des corps pedonculés. Z. Zllforsch 106: 220-231.

Menzel R, Greggers U, Smith A, Berger S, Brandt R, Brunke S, Bundrock G, Hülse S, Plümpe T, Schaupp F, Schüttler E, Stach S, Stindt J, Stollhoff N, Watzl S. 2005. Honey bees navigate according to a map-like spatial memory. Proc Natl Acad Sci USA 102:3040–3045.

Menzel R. 2014. The insect mushroom body, an experience-dependent recoding device. J Physiol Paris 108:84–95.

Merrill R et al. The diversification of *Heliconius* butterflies: what have we learned in 150 years? J Evol Biol. *in review*

Merrill R Naisbit RE, Mallet J, Jiggins CD. 2013. Ecological and genetic factors influencing the transition between host-use strategies in sympatric *Heliconius* butterflies. *J Evol Biol.* 26: 1959-1967.

Mery F, Kawecki TJ. 2004. An operating cost of learning in *Drosophila melanogaster*. Anim Behav 68:589–598.

Mizunami M, Weibrecht JM, Strausfeld NJ. 1998. Mushroom bodies of the cockroach: Their participation in place memory. J Comp Neurol 402:520–537.

Molina Y, O'Donnell S. 2007. Mushroom body volume is related to social aggression and ovary development in the paperwasp *Polistes instabilis*. Brain Behav Evol 70:137–144.

Montgomery SH, Ott SR. 2015. Brain composition in *Godyris zavaleta* , a diurnal butterfly, reflects an increased reliance on olfactory information. J Comp Neurol 523:869–891.

Mota T, Yamagata N, Giurfa M, Gronenberg W, Sandoz J-C. 2011. Neural organization and visual processing in the anterior optic tubercle of the honeybee brain. J Neurosci 31:11443–11456.

Müller F. 1879. Ituna and Thyridia: a remarkable case of mimicry in butterflies. Trans Entomol Soc Lond:20–29.

Murawski DA, Gilbert LE. 1986. Pollen flow in *Psiguria warscewiczii*: a comparison of *Heliconius* butterflies and hummingbirds. Oecologia 68:161–167.

Muscedere ML, Gronenberg W, Moreau CS, Traniello JF a. 2014. Investment in higher order central processing regions is not constrained by brain size in social insects. Proc Biol Sci 281:20140217.

Neuser K, Triphan T, Mronz M, Poeck B, Strauss R. 2008. Analysis of a spatial orientation memory in *Drosophila*. Nature 453:1244–1247.

Van Nouhuys S, Kaartinen R. 2008. A parasitoid wasp uses landmarks while monitoring potential resources. Proc Biol Sci 275:377–385.

O'Brien DM, Boggs CL, Fogel ML. 2003. Pollen feeding in the butterfly *Heliconius* charitonia: isotopic evidence for essential amino acid transfer from pollen to eggs. Proc Biol Sci 270:2631–2636.

O'Donnell S, Clifford MR, DeLeon S, Papa C, Zahedi N, Bulova SJ. 2013. Brain size and visual environment predict species differences in paper wasp sensory processing brain regions (hymenoptera: vespidae, polistinae). Brain Behav Evol 82:177–84.

Ofstad TA, Zuker CS, Reiser MB. 2011. Visual place learning in *Drosophila melanogaster*. Nature 474:204–207.

Ott SR, Rogers SM. 2010. Gregarious desert locusts have substantially larger brains with altered proportions compared with the solitarious phase. Proc Biol Sci 277:3087–96.

Ott SR. 2008. Confocal microscopy in large insect brains: zinc-formaldehyde fixation improves synapsin immunostaining and preservation of morphology in whole-mounts. J Neurosci Methods 172:220–30.

Pagel M. 1999. Inferring the historical patterns of biological evolution. Nature 401:877–84.

Park PJ, Bell MA. 2010. Variation of telencephalon morphology of the threespine stickleback (*Gasterosteus aculeatus*) in relation to inferred ecology. J Evol Biol 23:1261–1277.

Paulk AC, Dacks AM, Gronenberg W. 2009a. Color processing in the medulla of the bumblebee (Apidae: *Bombus impatiens*). J Comp Neurol 513:441–456.

Paulk AC, Dacks AM, Phillips-Portillo J, Fellous J-M, Gronenberg W. 2009b. Visual processing in the central bee brain. J Neurosci 29:9987–9999.

Penz CM, Krenn HW. 2000. Behavioral adaptations to pollen-feeding in *Heliconius* butterflies (Nymphalidaae, Heliconiinae): An experiment using *Lantana* flowers. J Insect Behav 13 :865–880.

Pfeiffer K, Homberg U. 2014. Organization and functional roles of the central complex in the insect brain. Annu Rev Entomol 59:165–84.

Pfeiffer K, Kinoshita M, Homberg U. 2005. Polarization-sensitive and light-sensitive neurons in two parallel pathways passing through the anterior optic tubercle in the locust brain. J Neurophysiol 94:3903–3915.

Pfeiffer K, Kinoshita M. 2012. Segregation of visual inputs from different regions of the compound eye in two parallel pathways through the anterior optic tubercle of the bumblebee (*Bombus ignitus*). J Comp Neurol 520:212–229.

Pfennig DW, Wund MA, Snell-Rood EC, Cruickshank T, Schlichting CD, Moczek AP. 2010. Phenotypic plasticity's impacts on diversification and speciation. Trends Ecol Evol 25:459–467.

Plath OE. 1934. Bumblebees and their Ways. London, UK. The Macmillan Company.

Pollen AA, Dobberfuhl AP, Scace J, Igulu MM, Renn SCP, Shumway CA, Hofmann H a. 2007. Environmental complexity and social organization sculpt the brain in Lake Tanganyikan cichlid fish. Brain Behav Evol 70:21–39.

Rath L, Giovanni Galizia C, Szyszka P. 2011. Multiple memory traces after associative learning in the honey bee antennal lobe. Eur J Neurosci 34:352–360.

Rehder V. 1989. Sensory pathways and motoneurons of the proboscis reflex in the suboesophageal ganglion of the honey bee. J Comp Neurol 279:499–513.

Rein K, Zöckler M, Mader MT, Grübel C, Heisenberg M. 2002. The *Drosophila* standard brain. Curr Biol 12:227–31.

Renwick JAA, Chew FS. 1994. Oviposition behavior in Lepidoptera. Annu Rev Entomol 39:377–400.

Rø H, Müller D, Mustaparta H. 2007. Anatomical organization of antennal lobe projection neurons in the moth *Heliothis virescens*. J Comp Neurol 500:658–75.

Rosenheim J a. 1987. Host location and exploitation by the cleptoparasitic wasp *Argochrysis armilla*: the role of learning (Hymenoptera: Chrysididae). Behav Ecol Sociobiol 21:401–406.

Rospars JP. 1983. Invariance and sex-specific variations of the glomerular organization in the antennal lobes of a moth, *Mamestra brassicae*, and a butterfly, *Pieris brassicae*. J Comp Neurol 220:80–96.

Safi K, Dechmann DKN. 2005. Adaptation of brain regions to habitat complexity: a comparative analysis in bats (Chiroptera). Proc Biol Sci 272:179–186.

Salcedo C. 2011. Pollen preference for *Psychotria sp*. is not learned in the passion flower butterfly, *Heliconius erato*. J Insect Sci 11:25.

Schildberger K. 1983. Local interneurons associated with the mushroom bodies and the central body in the brain of *Acheta domesticus*. Cell Tissue Res 230:573–586.

Schoonhoven LM. 1968. Chemosensory Bases of Host Plant Selection. Annu Rev Entomol 13:115–136.

Schürmann FW. 1970. Structure of the mushroom bodies of the insect brain. I. Synapses in the peduncle. Zeitschrift für Zellforsch und mikroskopische Anat (Vienna, Austria 1948) 103:365.

Seymoure B, McMillan WO, Rutowski RL. Corneal area and facet diameters in Longwing (*Heliconius*) butterflies vary with body size and sex but not light environment nor mimicry ring. *in review*.

Shumway CA. 2008. Habitat complexity, brain, and behavior. Brain Behav Evol 72:123–134.

Silva AK, Gonçalves GL, Moreira GRP. 2014. Larval feeding choices in heliconians: Induced preferences are not constrained by performance and host plant phylogeny. Anim Behav 89:155–162.

Sivinski J. 1989. Mushroom body development in nymphalid butterflies: A correlate of learning? J Insect Behav 2:277–283.

Sjöholm M, Sinakevitch I, Ignell R, Strausfeld NJ, Hansson BS. 2005. Organization of Kenyon cells in subdivisions of the mushroom bodies of a lepidopteran insect. J Comp Neurol 491:290–304.

Skiri HT, Rø H, Berg BG, Mustaparta H. 2005. Consistent organization of glomeruli in the antennal lobes of related species of Heliothine moths. J Comp Neurol 491:367–80.

Smiley JT. 1978. The host plant ecology of *Heliconius* butterflies in northeastern Costa Rica. PhD. University of Texas at Austin, Austin, Texas.

Smith AR, Seid MA, Jiménez LC, Wcislo WT. 2010. Socially induced brain development in a facultatively eusocial sweat bee *Megalopta genalis* (Halictidae). Proc Biol Sci 277:2157–2163.

Snell-Rood EC, Davidowitz G, Papaj DR. 2011. Reproductive tradeoffs of learning in a butterfly. Behav Ecol 22:291–302.

Snell-Rood EC, Papaj DR, Gronenberg W. 2009. Brain size: a global or induced cost of learning? Brain Behav Evol 73:111–28.

Snell-Rood EC. 2013. An overview of the evolutionary causes and consequences of behavioural plasticity. Anim Behav 85:1004–1011.

Stopfer M. 2014. ScienceDirect Central processing in the mushroom bodies. Curr Opin Insect Sci 6:99–103. A

Tamura K, Peterson D, Peterson N, Stecher G, Nei M, Kumar S. 2011. MEGA5: molecular evolutionary genetics analysis using maximum likelihood, evolutionary distance, and maximum parsimony methods. Mol Biol Evol 28:2731–9.

R Development Consortium. 2008. R: A language and environment for statistical computing. R Foundation for Statistical Computing, Vienna, Austria. ISBN 3-900051-07-0. URL http//wwwR-project.org.

Trautwein MD, Wiegmann BM, Beutel R, Kjer KM, Yeates DK. 2012. Advances in insect phylogeny at the dawn of the postgenomic era. Annu Rev Entomol 57:449–468.

Turner JRG. 1971. Experiments on the demography of tropical butterflies. II. Longevity and home-range behaviour in *Heliconius erato*. Biotropica 3:21–31.

Turner JRG. 1981. Adaptation and evolution in *Heliconius*: A defense of NeoDarwinism. Annu Rev Ecol Syst 12:99–121.

Warren AD, Davis KJ, Strangeland EM, Pelham JP, Grishin NV. 2013. Illustrated lists of American butterflies. http://butterfliesofamerica.com

Warton DI, Duursma RA., Falster DS, Taskinen S. 2012. smatr 3- an R package for estimation and inference about allometric lines. Methods Ecol Evol 3:257–259.

Wei H, el Jundi B, Homberg U, Stengl M. 2010. Implementation of pigment-dispersing factor-immunoreactive neurons in a standardized atlas of the brain of the cockroach *Leucophaea maderae*. J Comp Neurol 518:4113–33.

Whiting BA, Barton RA. 2003. The evolution of the cortico-cerebellar complex in primates: Anatomical connections predict patterns of correlated evolution. J Hum Evol 44:3–10.

Withers G, Day NF, Talbot EF, Dobson HEM, Wallace CS. 2008. Experience-dependent plasticity in the mushroom bodies of the solitary bee *Osmia lignaria* (Megachilidae). Dev Neurobiol 68:73–82.

Withers GS, Fahrbach SE, Robinson GE. 1993. Selective neuroanatomical plasticity and division of labour in the honeybee. Nature364:238–40.

Zars T. 2000. Behavioral functions of the insect mushroom bodies. Curr Opin Neurobiol 10:790–795.

Abbreviations

AL	antennal lobe
aMe	accessory medulla
AN	antennal nerve
AOTu	anterior optic tubercule
CB	central body
CBL	lower central body
CBU	upper central body
CFN	central fibrous neuropil of *AL*
DMSO	dimethyl suphoxide
Glom	glomeruli
HBS	HEPES-buffered saline
iMe	inner medulla
iRim	inner rim of the lamina
La	lamina
LAL	lateral accessory lobes
Lo	lobula
LoP	lobula plate
LU	lower unit of *AOTu*
MB	mushroom body
MB-ca	mushroom body calyx
MB-lo	mushroom body lobes
MB-pe	mushroom body peduncle
MB-lo+pe	mushroom body lobes and peduncle combined
MBr	midbrain
Me	medulla
MGC	macro-glomeruli complex
NGS	normal goat serum
no	noduli
NU	nodule unit of *AOTu*
oMe	outer medulla
OR	olfactory receptor
OGC	optic glomerular complex
PA	pyrrolizidine alkaloids
PB	protocerebral bridge
PC	principal component
POTu	posterior optic tubercle
rMid	rest of midbrain
SP	strap of *AOTu*
UU	upper unit of *AOTu*
ZnFA	Zinc-Formaldehyde solution

Figure Legends

Figure 1: Overview of the anatomy of the *Heliconius* brain.

3D models of *H. erato* (**A–G**) and *H. hecale* (**A'–G'**). **B–D** and **B'–D':** Volume rendering of synapsin immunofluorescence showing the surface morphology of the brain neuropil from the anterior (A/A'), posterior (B/B'), and dorsal (C/C') view. **E–G** and **E'–G':** Surface reconstructions of the major neuropil compartments from the anterior (D), posterior (E), and dorsal (F) view. Neuropil in yellow-orange: visual neuropil, green: central complex, blue: antennal lobes, red: mushroom bodies. See Figures 2–4 for further anatomical detail. The individuals displayed are male. Images in A/A' are from Warren et al. (2013). Scale bars = 25 mm in A/A'; 500 µm in B–D/B'–D'.

Figure 2: Anatomy of the sensory neuropils.

Images A–H are from male *H. hecale*. **A:** Surface reconstructions of the optic lobe neuropils viewed from anterior (left image) and posterior (right image). They comprise the lamina (La), the medulla (Me), and accessory medulla (aMe), the lobula (Lo), the lobula plate (LoP) and the optic glomerulus (OG). **B:** Surface reconstruction of the optic glomerulus (OG) viewed along the anterior-posterior axis (top) and an anterior view (bottom)**. C:** Surface reconstruction of the anteriot optic tubercle (AOTu)**. D–J:** Synapsin immunofluorescence in single confocal sections of the optic lobe of *H. hecale*. **D:** Horizontal section showing all four major optic lobe neuropils (La, Me, Lo, LoP). **E:** Frontal section showing the inner rim (iRim) of the lamina, a thin layer on its inner surface that is defined by intense synapsin immunofluorescence. Synapsin immunostaining also reveals the laminated structure of the medulla with two main subdivisions, the outer and inner medulla (oMe, iMe). **F:** The OG is located medially to the Lo; frontal section, the midbrain (MBr) occupies the left half of the frame. **G,H:** Frontal sections showing a small, irregular neuropil (ir) observed running from the anterior-ventral boundary of the aME as in *D. plexippus* (Heinze and Reppert, 2012).

Figure 3: Anatomy of the antennal lobe

A: 3D reconstruction of individual antennal lobe (AL) glomeruli superimposed on a volume rendering of the anterior surface of the midbrain. **B:** Synapsin immunofluorescence in a single frontal confocal section showing the glomeruli (Glom) surrounding the central fibrous neuropil (CFN). Images A–B are from male *H. hecale.* **C,D:** Allometric grade-shifts between Glom (circles) or CFN (triangles) volume and unsegmented midbrain volume (C), and between Glom and CFN volume (D) in *G. zavaleta* (solid blue), *H. erato* (black filled with red) and *H. hecale* (orange filled with yellow). Scale bars = 500 µm in A; 50 µm in B,C,G,H; 100 µm in B–F, J; 200 µm in I.

Figure 4: Anatomy of the central complex

A/A': Surface reconstruction of the central complex from an anterolateral (A) and oblique posteroventral (A') view, showing the upper and lower subunit of the central body (CBU, CBL), the noduli (No), the protocerebral bridge (PB) and posterior optic tubercles (POTu). **B–G:** Synapsin immunofluorescence in single confocal sections. **B:** Horizontal section showing the upper and lower subunit of the CB in relation to the antennal lobes (AL) and the calyx (MB-ca) and pedunculus (MB-pe) of the mushroom body. **C,D:** Frontal confocal sections at the level of the CBL (C) and CBU (D); the CB subunits are flanked by the profiles of the vertically running MB-pe on either side. **E:** Frontal section showing the location of the PB ventrally to the MB-ca. **F:** POTu positioned ventrally to the MB-ca in a frontal section. **G:** Frontal section showing position of the paired No ventrally to CBL and CBU. All images are from a male *H. hecale.* Scale bars = 100 µm in B–D, G; 50 µm in E,F.

Figure 5: Anatomy of the mushroom body

A–C: Surface reconstruction of the mushroom body viewed (A), orthogonal to the anterior-posterior axis from a medial vantage point level with the peduncle; (B), from anterior; and (C), from posterior. The main components are the calyx (MB-ca) shown in dark red, and the peduncule (MB-pe) and lobes (MB-lo) shown in bright red. A Y-tract, shown in magenta, runs parallel and slightly medial to the MB-pe. **D–K:** Synapsin immunofluorescence in individual confocal sections. **D:** anterior view of the midbrain showing the MB-lo, an asterik indicates the probably ventral lobe, otherwise the individual lobes and loblets of the MB-lo are fused. **E:** Frontal section at a

posterior level near the end of the MB-pe, showing the profiles of the MB-ca with its zonation into an outer and a medial ring. **F,G** and **J,K**: Horizontal confocal sections through the midbrain at increasing depths from dorsal towards ventral, showing MB structure in relation to neighboring neuropil: the anterior optic tubercle (AOTu in F,G); the antennal lobe (AL in G,J); and the central body upper division (CBU in K). **H:** An example of a female *H. erato* where the MB-ca is deformed due expansion into the optic lobe and constriction (C) at the optic stalk by the neural sheath surrounding the brain. **I:** Pitted surface of the MB-ca in a very posterior tangential horizontal section. The pitting is related to what appear to be columnar domains within the calyx neuropil (*cf.* MB-ca in J,K,M). **L:** Areas of intense synapsin staining in the optic stalk (OS*); Lo, lobula; OG, optic glomerulus. **M:** Frontal section near the base of the calyx (MB-ca) showing a satellite neuropil (sat.) located near to the MB-pe. **N:** A Y-tract runs parallel with, and dorsally and slightly medially to the MB-pe; both are seen in profile in this frontal section. **O:** A fiber bundle (fb) connected to the AOTu running near the junction between the MB-pe and MB-lo. With the exception of I, all images are from a male *H. hecale.* Scale bars A-G, J-K = 200 µm, H-I, L-O = 100 µm.

Figure 6: Age and environment dependent growth of the mushroom bodies

Surface reconstruction of the mushroom body viewed along the anterior-posterior axis for wild-caught, old and young insectary-reared individuals of *H. erato* (**A**) and *H. hecale* (**A'**). Representative individuals were chosen as those closest to the group mean volume. Scale bar = 200 µm. **B-C/B'-C':** allometric relationships between MB-lo+pe (B/B'), or MB-ca (C/C'),and the volume of the unsegmented midbrain (rMid) for *H. erato* (B/C) and *H. hecale* (B'/C'). Data for wild caught individuals are in green, data for old insectary-reared individuals in dark blue, and data for young insectary-reared individuals are in light blue. Allometric slopes for each group are shown, the slope, intercepts and major-axis means are compared in Table 2, 3.

Figure 7: Age and environment dependent growth of brain components

A,D: Comparisons of raw volumes of total neuropil, total OL neuropil, total midbrain neuropil between wild-caught, old and young insectary-reared individuals of *H. erato* (A) and *H. hecale* (D). Significance of pair-wise comparisons are shown along the x-axis (young-old = orange; old-wild = dark red; n.s. = $p>0.05$, * = $p<0.05$, ** = $p<0.01$, *** = $p < 0.001$). **B:** Allometric scaling of LoP in *H. erato*. **C:** Allometric

scaling of PB in *H. erato*. **E:** Allometric scaling of OG in *H. hecale*. **F:** Allometric scaling of CB in *H. hecale*. Note in E and F the shifts in allometry occur along the x-axis, this is explained by the large difference in unsegmented midbrain volume observed between wild-caught and old insectary-reared individuals in *H. hecale* as displayed in D.

Figure 8: Divergence in brain structure between *H. erato* and *H. hecale.*

A–C: Species differences in brain-body scaling between *H. erato* (red) and *H. hecale* (orange). Grade-shifts towards larger neuropil volume relative to body length are seen for total neuropil (A) but are mainly driven by OL neuropil (B) rather than midbrain neuropil (C). **D:** Discriminant Function analysis of segmented neuropil volumes and the unsegmented midbrain volume separates wild individuals of the two species along a single axis (yellow, orange ring: wild *H. hecale;* red, black ring: wild *H. erato*). **E, F:** DFA including wild and old insectary-reared individuals of both species (solid orange = old insectary-reared *H. hecale*; solid black: old insectary-reared *H. erato*). E displays DF1 vs. DF2 to illustrate that DF1 accounts for the most variation between species, F displays DF2 vs. DF3 to illustrate that these axes separate wild and old insectary-reared individuals of the same species.

Figure 9: Divergence in brain structure across Lepidoptera, and in mushroom body size across insects.

A: Phylogenetic relationships of Lepidoptera (red branches) and other insects (grey branches) for which comparable data are available. Branches are not drawn proportional to divergence dates, numbers refer to labels in panel E. **B,C:** Principal Component analysis of segmented neuropil volumes, corrected for allometric scaling with the unsegmented midbrain and phylogeny. **B:** Analysis using all neuropil. **C:** Analysis excluding the optic lobe neuropil. Species data points are indicated by the first letter of their genus and species name: *D.p = Danaus plexippus*; *H.e = Heliconius erato*; *H.h = H. hecale*; *G.z = Godyris zavaleta*; *H.v = Heliothis virescens*; *M.s = Manduca sexta*. **D:** The proportion of the midbrain occupied by MB-ca (dark red) and MB-lo+pe (light red) in four butterflies, and two other insects with fully comparable data. **E:** Across a wider sample of insects (shown in A), when expressed as a percentage of total volume of OL, AL, CB and MB, *Apis mellifera* (solid blue) and *Heliconius* (solid red) stand out as having expanded mushroom bodies, correcting for

the size of the optic neuropil, compared to other Lepidoptera (unfilled red circles) and other insects (unfilled blue circles). The line was fitted by PGLS. All insect images in A are from Wikimedia commons and were released under the Creative Commons License, except *Heliconius* (see Fig. 1).

Tables

Table 1: Neuropil volumes and body size of A) *H. erato* and B) *H. hecale*

Table 2: Comparisons between old (O) and young (Y) insectary-reared individuals for A) *H. erato* and B) *H. hecale. r* is the effect size. DI indicates the group with a higher value of α, β or fitted axis mean.

Table 3: Comparisons between wild caught (W) and old insectary-reared individuals for A) *H. erato* and B) *H. hecale. r* is the effect size. DI indicates the group with a higher value of α, β or fitted axis mean.

Table 4: Comparisons between *H. erato* and *H. hecale* for A) wild caught and B) old insectary-reared individuals. *r* is the effect size. DI indicates the species with a higher value of α, β or fitted axis mean.

Table 5: Discriminant function analysis of variation between wild and old insectary-reared *H. erato* and *H. hecale.* A) Canonical discrimant function coefficitions for DF1-3. B) Disrciminant function statistics. C) Results of a MANOVA of DF1-3 to test for associations with species, group, and species-group interactions.

Table 6: Loadings on Principal Components Analysis of the relative size of brain components across six Lepidoptera.

Table 1

A) *H. erato*

	wild caught				*old insectary reared*		*young insectary reared*	
	mean (*n* = 10)	**SD**	**Rel. SD (%)**	**% total Neuropil**	**mean (*n* = 10)**	**SD**	**mean (*n* = 10)**	**SD**
Body mass (g)	0.093	0.017	19.999	-	0.074	0.014	0.088	0.019
Body length (mm)	23.833	1.426	5.983	-	23.095	1.773	22.671	0.951
Wing span (mm)	71.408	3.278	4.591	-	69.744	4.12	68.786	2.55
Lamina	7.409E+07	1.052E+07	14.192	13.459	6.95E+07	1.61E+07	5.49E+07	1.25E+07
Medulla	2.396E+08	3.617E+07	15.094	43.523	2.45E+08	2.76E+07	1.90E+08	3.32E+07
Accessory medulla	1.633E+05	3.609E+04	22.094	0.030	1.59E+05	4.61E+04	9.77E+04	1.93E+04
Inner lobula	2.630E+07	4.203E+06	15.984	4.777	2.79E+07	2.89E+06	2.07E+07	4.32E+06
Lobula plate	1.393E+07	2.083E+06	14.952	2.531	1.35E+07	2.22E+06	1.04E+07	2.07E+06
OG	1.054E+06	2.400E+05	22.769	0.191	1.05E+06	2.42E+05	8.85E+05	2.26E+05
Antennal lobes	1.185E+07	2.450E+06	20.671	2.153	1.19E+07	2.49E+06	7.72E+06	1.10E+06
AOTu	2.199E+06	4.535E+05	20.618	0.400	2.26E+06	3.28E+05	1.52E+06	3.27E+05
MB calyx	4.672E+07	9.290E+06	19.886	8.486	4.50E+07	1.22E+07	2.79E+07	5.75E+06
MB peduncle	6.043E+06	1.109E+06	18.343	1.098	6.15E+06	1.35E+06	5.57E+06	1.58E+06
MB lobes	2.267E+07	5.812E+06	25.641	4.118	2.17E+07	4.26E+06	1.28E+07	2.31E+06
Central body lower	3.017E+05	5.189E+04	17.198	0.055	2.83E+05	6.00E+04	2.24E+05	3.81E+04
Central body upper	1.180E+06	1.788E+05	15.153	0.214	1.17E+06	2.57E+05	8.90E+05	1.36E+05
Noduli	2.966E+04	1.146E+04	38.631	0.005	3.09E+04	1.64E+04	3.16E+04	8.46E+03
Protocerebral bridge	2.120E+05	4.804E+04	22.658	0.039	1.96E+05	5.04E+04	1.39E+05	2.02E+04
POTu	4.213E+04	9.976E+03	23.681	0.008	4.20E+04	1.43E+04	2.73E+04	7.93E+03
Total midbrain	1.954E+08	3.365E+07	17.222	35.490	2.04E+08	2.70E+07	1.39E+08	2.28E+07

Table 1 continued
B) *H. hecale*

	wild caught				*old insectary reared*		*young insectary reared*	
	mean (*n* = 10)	**SD**	**Rel. SD (%)**	**% total Neuropil**	**mean (*n* = 9)**	**SD**	**mean (*n* = 10)**	**SD**
Body mass (g)	0.163	0.025	15.317	-	0.154	0.046	0.171	0.047
Body length (mm)	29.693	3.097	10.431	-	28.189	3.0631	29.206	2.75
Wing span (mm)	88.129	8.004	9.082	-	80.6	7.134	86.34	8.012
Lamina	9.751E+07	1.826E+07	18.721	13.939	9.39E+07	2.17E+07	9.64E+07	1.50E+07
Medulla	2.986E+08	5.342E+07	17.888	42.689	2.48E+08	3.81E+07	2.42E+08	3.66E+07
Accessory medulla	1.660E+05	2.951E+04	17.782	0.024	1.40E+05	2.80E+04	1.38E+05	3.67E+04
Inner lobula	3.056E+07	5.630E+06	18.422	4.369	2.80E+07	4.64E+06	2.45E+07	5.06E+06
Lobula plate	1.648E+07	2.972E+06	18.031	2.356	1.45E+07	2.45E+06	1.27E+07	2.53E+06
OG	1.099E+06	3.396E+05	30.894	0.157	9.93E+05	2.12E+05	9.24E+05	2.10E+05
Antennal lobes	1.216E+07	2.056E+06	16.905	1.739	1.09E+07	1.34E+06	9.36E+06	1.59E+06
AOTu	2.572E+06	6.144E+05	23.891	0.368	2.30E+06	4.46E+05	2.02E+06	3.76E+05
MB calyx	5.271E+07	1.611E+07	30.569	7.534	3.60E+07	7.49E+06	2.60E+07	7.48E+06
MB peduncle	6.680E+06	1.525E+06	22.834	0.955	5.92E+06	1.30E+06	4.91E+06	1.39E+06
MB lobes	2.421E+07	6.279E+06	25.930	3.461	1.79E+07	3.56E+06	1.32E+07	3.51E+06
Central body lower	3.109E+05	6.362E+04	20.467	0.044	2.91E+05	7.15E+04	2.47E+05	3.74E+04
Central body upper	1.093E+06	2.026E+05	18.541	0.156	1.16E+06	2.05E+05	9.65E+05	1.79E+05
Noduli	4.207E+04	1.713E+04	40.730	0.006	3.34E+04	8.35E+03	3.06E+04	1.28E+04
Protocerebral bridge	2.424E+05	5.657E+04	23.335	0.035	2.00E+05	3.09E+04	1.64E+05	1.75E+04
POTu	4.183E+04	1.257E+04	30.057	0.006	3.74E+04	8.47E+03	3.20E+04	8.27E+03
Total midbrain	2.551E+08	6.253E+07	24.513	36.465	1.82E+08	2.28E+07	1.50E+08	2.25E+07

Table 2

A) *H. erato*

	Volume			Scaling coefficient (β)			Intercept (α)			Major Axis Shift		
	t17	**p**	**r (DI)**	**Likelihood Ratio**	**p**	**r (DI)**	**Wald χ2**	**p**	**r (DI)**	**Wald χ2**	**p**	**r (DI)**
Lamina	2.432	0.026	0.508 (O)	2.019	0.155	-	2.895	0.089	-	13.196	0.000	0.833 (O)
Medulla	4.118	0.001	0.707 (O)	0.090	0.765	-	1.127	0.288	-	19.405	0.000	1.000 (O)
Accessory medulla	3.802	0.001	0.678 (O)	3.976	0.046	0.458 (O)	-	-	-	-	-	-
Inner lobula	4.173	0.001	0.711 (O)	0.246	0.620	-	1.587	0.208	-	20.284	0.000	1.000 (O)
Lobula plate	3.266	0.005	0.621 (O)	0.523	0.470	-	3.802	0.051	-	19.034	0.000	1.000 (O)
OG	1.412	0.176	-	0.385	0.535	-	5.694	0.017	0.547 (Y)	10.622	0.001	0.748 (O)
Antennal lobes	5.080	0.000	0.776 (O)	4.169	0.041	-	0.214	0.644	-	27.584	0.000	1.000 (O)
AOT	5.192	0.000	0.783 (O)	0.109	0.741	-	0.123	0.726	-	26.321	0.000	1.000 (O)
MB calyx	4.050	0.001	0.701 (O)	3.679	0.055	-	1.607	0.205	-	19.177	0.000	1.000 (O)
MB lobes+peduncle	4.806	0.000	0.759 (O)	0.963	0.326	-	0.373	0.541	-	23.250	0.000	1.000 (O)
CB L+U	3.272	0.004	0.622 (O)	2.364	0.124	-	1.807	0.179	-	16.530	0.000	0.933 (O)
Protocerebral bridge	3.169	0.006	0.609 (O)	5.996	0.014	0.562 (O)	-	-	-	-	-	-
POTu	2.772	0.013	0.558 (O)	1.539	0.215	-	4.124	0.042	0.466 (Y)	14.953	0.000	0.887 (O)
Total Mid	4.192	0.001	0.713 (O)	-	-	-	-	-	-	-	-	-
rMid	5.771	0.000	0.814 (O)	-	-	-	-	-	-	-	-	-
Total OL	5.076	0.000	0.776 (O)	-	-	-	-	-	-	-	-	-
Total neuropil	5.153	0.000	0.781 (O)	-	-	-	-	-	-	-	-	-

B) *H. hecale*

	Volume			Scaling coefficient (β)			Intercept (α)			Major Axis Shift		
	t18	**p**	**r (DI)**	**Likelihood Ratio**	**p**	**r (DI)**	**Wald χ2**	**p**	**r (DI)**	**Wald χ2**	**p**	**r (DI)**
Lamina	-0.424	0.677	-	1.866	0.172	-	11.902	0.001	0.771 (Y)	1.043	0.307	-
Medulla	0.333	0.743	-	0.494	0.482	-	21.674	0.000	1.000 (Y)	1.971	0.160	-
Accessory medulla	0.238	0.814	-	0.094	0.759	-	3.044	0.081	-	3.088	0.079	-
Inner lobula	1.538	0.141	-	0.002	0.961	-	3.544	0.060	-	4.501	0.034	0.474 (O)
Lobula plate	1.683	0.110	-	0.066	0.797	-	1.577	0.209	-	5.031	0.025	0.502 (O)
OG	0.617	0.545	-	0.266	0.606	-	4.408	0.036	0.470 (Y)	3.045	0.081	-
						-						
Antennal lobes	2.418	0.026	-	1.795	0.180	-	2.396	0.122	-	6.451	0.011	0.570 (O)
AOT	1.496	0.152	-	0.101	0.751	-	2.166	0.141	-	4.656	0.031	0.483 (O)
MB calyx	3.177	0.005	0.599 (O)	0.283	0.595	-	0.104	0.747	-	9.166	0.002	0.677 (O)
MB lobes+peduncle	2.707	0.014	0.538 (O)	0.147	0.702	-	0.015	0.902	-	7.594	0.006	0.616 (O)
CB L+U	2.218	0.040	0.463 (O)	3.291	0.070	-	0.859	0.354	-	7.221	0.007	0.601 (O)
Protocerebral bridge	3.291	0.004	0.613 (O)	1.043	0.307	-	0.172	0.678	-	9.448	0.002	0.687 (O)
POTu	1.494	0.153	-	0.078	0.780	-	0.736	0.391	-	6.292	0.012	0.561 (O)
Total Mid	3.054	0.007	0.584 (O)	-	-	-	-	-	-	-	-	-
rMid	2.854	0.011	0.558 (O)	-	-	-	-	-	-	-	-	-
Total OL	0.280	0.783	-	-	-	-	-	-	-	-	-	-
Total neuropil	1.082	0.293	-	-	-	-	-	-	-	-	-	-

Table 3

A) *H. erato*

	Volume			Scaling coefficient (β)			Intercept (α)			Major Axis Shift		
	t17	**p**	**r (DI)**	**Likelihood Ratio**	**p**	**r (DI)**	**Wald χ2**	**p**	**r (DI)**	**Wald χ2**	**p**	**r (DI)**
Lamina	0.892	0.385	-	3.685	0.055	-	3.605	0.058	-	0.210	0.646	-
Medulla	-0.426	0.676	-	0.269	0.604	-	2.056	0.152	-	1.269	0.260	-
Accessory medulla	0.359	0.724	-	5.150	0.023	0.521 (O)	-	-	-	-	-	-
Inner lobula	-1.056	0.306	-	0.283	0.595	-	1.004	0.316	-	1.999	0.157	-
Lobula plate	0.430	0.673	-	4.963	0.026	0.511 (O)	-	-	-	-	-	-
OG	0.116	0.909	-	2.148	0.143	-	2.055	0.152	-	0.848	0.357	-
Antennal lobes	-0.035	0.972	-	1.695	0.193	-	2.269	0.132	-	0.899	0.343	-
AOT	-0.490	0.631	-	0.483	0.487	-	1.318	0.251	-	1.456	0.227	-
MB calyx	0.511	0.616	-	5.833	0.016	0.554 (O)	-	-	-	-	-	-
MB lobes+peduncle	0.239	0.814	-	0.714	0.398	-	4.418	0.036	0.482 (W)	7.594	0.006	0.632 (W)
CB L+U	0.394	0.699	-	4.272	0.039	0.474 (O)	-	-	-	-	-	-
Protocerebral bridge	0.845	0.410	-	4.413	0.036	0.482 (O)	-	-	-	-	-	-
POTu	0.196	0.847	-	3.726	0.054	-	2.730	0.098	-	0.905	0.341	-
Total Mid	-0.732	0.474	-	-	-	-	-	-	-	-	-	-
rMid	-1.787	0.092	-	-	-	-	-	-	-	-	-	-
Total OL	-0.123	0.904	-	-	-	-	-	-	-	-	-	-
Total neuropil	-0.432	0.671	-	-	-	-	-	-	-	-	-	-

B) *H. hecale*

	Volume			Scaling coefficient (β)			Intercept (α)			Major Axis Shift		
	t18	**p**	**r (DI)**	**Likelihood Ratio**	**p**	**r (DI)**	**Wald χ2**	**p**	**r (DI)**	**Wald χ2**	**p**	**r (DI)**
Lamina	0.437	0.667	-	6.725	0.010	0.580 (O)	-	-	-	-	-	-
Medulla	2.293	0.034	0.475 (W)	9.165	0.002	0.677 (O)	-	-	-	-	-	-
Accessory medulla	1.898	0.074	-	3.728	0.054	-	1.463	0.227	-	8.056	0.005	0.688 (W)
Inner lobula	1.017	0.322	-	9.760	0.002	0.699 (O)	-	-	-	-	-	-
Lobula plate	1.609	0.125	-	6.081	0.014	0.551 (O)	-	-	-	-	-	-
OG	0.614	0.547	-	4.262	0.039	0.462 (O)	-	-	-	-	-	-
Antennal lobes	1.519	0.146	-	7.095	0.008	0.596 (O)	-	-	-	-	-	-
AOT	1.088	0.291	-	3.938	0.047	0.444 (O)	-	-	-	-	-	-
MB calyx	3.126	0.006	0.593 (W)	1.657	0.198	-	0.395	0.530	-	10.432	0.001	0.722 (W)
MB lobes+peduncle	2.536	0.021	0.513 (W)	3.759	0.053	-	1.603	0.205	-	8.811	0.003	0.664 (W)
CB L+U	-0.446	0.661	-	1.665	0.197	-	11.013	0.001	0.742 (O)	2.385	0.122	-
Protocerebral bridge	1.919	0.071	-	5.043	0.025	0.502 (O)	-	-	-	-	-	-
POTu	0.551	0.588	-	5.420	0.020	0.521 (O)	-	-	-	-	-	-
Total Mid	3.658	0.002	0.653 (W)	-	-	-	-	-	-	-	-	-
rMid	3.417	0.003	0.627 (W)	-	-	-	-	-	-	-	-	-
Total OL	1.728	0.101	-	-	-	-	-	-	-	-	-	-
Total neuropil	2.553	0.020	0.516 (W)	-	-	-	-	-	-	-	-	-

Table 3

A) *H. erato*

	Volume			Scaling coefficient (β)			Intercept (α)			Major Axis Shift		
	t17	**p**	**r (DI)**	**Likelihood Ratio**	**p**	**r (DI)**	**Wald χ2**	**p**	**r (DI)**	**Wald χ2**	**p**	**r (DI)**
Lamina	0.892	0.385	-	3.685	0.055	-	3.605	0.058	-	0.210	0.646	-
Medulla	-0.426	0.676	-	0.269	0.604	-	2.056	0.152	-	1.269	0.260	-
Accessory medulla	0.359	0.724	-	5.150	0.023	0.521 (O)	-	-	-	-	-	-
Inner lobula	-1.056	0.306	-	0.283	0.595	-	1.004	0.316	-	1.999	0.157	-
Lobula plate	0.430	0.673	-	4.963	0.026	0.511 (O)	-	-	-	-	-	-
OG	0.116	0.909	-	2.148	0.143	-	2.055	0.152	-	0.848	0.357	-
Antennal lobes	-0.035	0.972	-	1.695	0.193	-	2.269	0.132	-	0.899	0.343	-
AOT	-0.490	0.631	-	0.483	0.487	-	1.318	0.251	-	1.456	0.227	-
MB calyx	0.511	0.616	-	5.833	0.016	0.554 (O)	-	-	-	-	-	-
MB lobes+peduncle	0.239	0.814	-	0.714	0.398	-	4.418	0.036	0.482 (W)	7.594	0.006	0.632 (W)
CB L+U	0.394	0.699	-	4.272	0.039	0.474 (O)	-	-	-	-	-	-
Protocerebral bridge	0.845	0.410	-	4.413	0.036	0.482 (O)	-	-	-	-	-	-
POTu	0.196	0.847	-	3.726	0.054	-	2.730	0.098	-	0.905	0.341	-
Total MB	-0.732	0.474	-	-	-	-	-	-	-	-	-	-
uMid	-1.787	0.092	-	-	-	-	-	-	-	-	-	-
Total OL	-0.123	0.904	-	-	-	-	-	-	-	-	-	-
Total neuropil	-0.432	0.671	-	-	-	-	-	-	-	-	-	-

B) *H. hecale*

	Volume			Scaling coefficient (β)			Intercept (α)			Major Axis Shift		
	t18	**p**	**r (DI)**	**Likelihood Ratio**	**p**	**r (DI)**	**Wald χ2**	**p**	**r (DI)**	**Wald χ2**	**p**	**r (DI)**
Lamina	0.437	0.667	-	6.725	0.010	0.580 (O)	-	-	-	-	-	-
Medulla	2.293	0.034	0.475 (W)	9.165	0.002	0.677 (O)	-	-	-	-	-	-
Accessory medulla	1.898	0.074	-	3.728	0.054	-	1.463	0.227	-	8.056	0.005	0.688 (W)
Inner lobula	1.017	0.322	-	9.760	0.002	0.699 (O)	-	-	-	-	-	-
Lobula plate	1.609	0.125	-	6.081	0.014	0.551 (O)	-	-	-	-	-	-
OG	0.614	0.547	-	4.262	0.039	0.462 (O)	-	-	-	-	-	-
Antennal lobes	1.519	0.146	-	7.095	0.008	0.596 (O)	-	-	-	-	-	-
AOT	1.088	0.291	-	3.938	0.047	0.444 (O)	-	-	-	-	-	-
MB calyx	3.126	0.006	0.593 (W)	1.657	0.198	-	0.395	0.530	-	10.432	0.001	0.722 (W)
MB lobes+peduncle	2.536	0.021	0.513 (W)	3.759	0.053	-	1.603	0.205	-	8.811	0.003	0.664 (W)
CB L+U	-0.446	0.661	-	1.665	0.197	-	11.013	0.001	0.742 (O)	2.385	0.122	-
Protocerebral bridge	1.919	0.071	-	5.043	0.025	0.502 (O)	-	-	-	-	-	-
POTu	0.551	0.588	-	5.420	0.020	0.521 (O)	-	-	-	-	-	-
Total MB	3.658	0.002	0.653 (W)	-	-	-	-	-	-	-	-	-
uMid	3.417	0.003	0.627 (W)	-	-	-	-	-	-	-	-	-
Total OL	1.728	0.101	-	-	-	-	-	-	-	-	-	-
Total neuropil	2.553	0.020	0.516 (W)	-	-	-	-	-	-	-	-	-

Table 4

A) Wild

	Volume			Scaling coefficient (β)			Intercept (α)			Major Axis Shift		
	t18	p	r (DI)	Likelihood Ratio	p	r (DI)	Wald χ2	p	r (DI)	Wald χ2	p	r (DI)
Lamina	3.268	0.004	0.610 (Hh)	0.072	0.789	-	0.095	0.758	-	11.283	0.001	0.751 (Hh)
Medulla	2.713	0.014	0.539 (Hh)	1.256	0.262	-	1.311	0.252	-	9.069	0.003	0.673 (Hh)
Accessory medulla	0.217	0.831	-	1.608	0.205	-	7.737	0.005	0.622 (He)	3.748	0.053	-
Inner lobula	1.817	0.086	-	0.998	0.318	-	4.759	0.029	0.488 (He)	6.704	0.010	0.579 (Hh)
Lobula plate	2.200	0.041	-	1.883	0.170	-	4.924	0.026	0.496 (He)	7.685	0.006	0.620 (Hh)
OG	0.136	0.893	-	0.021	0.886	-	16.729	0.000	0.915 (He)	3.203	0.074	-
Antennal lobes	0.390	0.701	-	7.367	0.007	0.607 (He)	-	-	-	-	-	-
AOT	1.550	0.139	-	1.227	0.268	-	9.657	0.002	0.695 (He)	6.117	0.013	0.553 (Hh)
MB calyx	0.863	0.400	-	0.000	0.995	-	5.405	0.020	0.520 (He)	4.798	0.028	0.490 (Hh)
MB lobes+peduncle	0.683	0.504	-	1.189	0.275	-	6.934	0.008	0.589 (He)	4.608	0.032	0.480 (Hh)
CB L+U	-0.866	0.398	-	0.164	0.686	-	9.685	0.002	0.696 (He)	2.260	0.133	-
Protocerebral bridge	1.262	0.223	-	2.869	0.090	-	1.436	0.231	-	6.571	0.010	0.573 (Hh)
POTu	-0.251	0.804	-	2.952	0.086	-	3.166	0.075	-	4.390	0.036	0.469 (Hh)
Total Mid	2.713	0.014	0.539 (Hh)	-	-	-	-	-	-	-	-	-
rMid	3.582	0.002	0.645 (Hh)	-	-	-	-	-	-	-	-	-
Total OL	2.866	0.010	0.560 (Hh)	-	-	-	-	-	-	-	-	-
Total neuropil	2.977	0.008	0.574 (Hh)	-	-	-	-	-	-	-	-	-

B) Old insectary-reared

	Volume			Scaling coefficient (β)			Intercept (α)			Major Axis Shift		
	t17	p	r (DI)	Likelihood Ratio	p	r (DI)	Wald χ2	p	r (DI)	Wald χ2	p	r (DI)
Lamina	2.949	0.009	0.582 (Hh)	0.015	0.902	-	14.433	0.000	0.872 (Hh)	0.488	0.485	-
Medulla	0.358	0.725	-	0.454	0.501	-	5.089	0.024	0.518 (Hh)	0.561	0.454	-
Accessory medulla	-0.395	0.697	-	1.634	0.201	-	0.167	0.683	-	1.679	0.195	-
Inner lobula	-0.480	0.637	-	1.886	0.170	-	4.099	0.043	-	0.548	0.459	-
Lobula plate	1.162	0.261	-	0.088	0.767	-	7.951	0.005	0.647 (Hh)	0.069	0.793	-
OG	-0.515	0.613	-	0.038	0.846	-	0.564	0.453	-	1.060	0.303	-
Antennal lobes	-1.329	0.201	-	2.557	0.110	-	0.001	0.974	-	1.155	0.283	-
AOT	0.064	0.950	-	0.133	0.715	-	1.112	0.292	-	0.621	0.431	-
MB calyx	-1.567	0.134	-	1.276	0.259	-	0.229	0.633	-	2.724	0.099	-
MB lobes+peduncle	-1.961	0.066	-	0.000	0.991	-	0.195	0.659	-	2.710	0.100	-
CB L+U	-0.378	0.710	-	1.751	0.186	-	3.937	0.047	0.455 (Hh)	0.151	0.698	-
Protocerebral bridge	-0.188	0.853	-	3.341	0.068	-	3.601	0.058	-	0.195	0.659	-
POTu	-0.429	0.673	-	1.532	0.216	-	0.372	0.542	-	1.329	0.249	-
Total Mid	-2.177	0.043	0.467 (He)	-	-	-	-	-	-	-	-	-
rMid	-1.391	0.181	-	-	-	-	-	-	-	-	-	-
Total OL	1.158	0.262	-	-	-	-	-	-	-	-	-	-

Total neuropil	0.145	0.886	-	-	-	-	-	-	-	-	-	-	-

Table 5

A) Canonical discriminant function coefficients

Neuropil	DF 1	DF 2	DF 3
rMid	1.716	0.892	-1.404
aME	-0.177	-0.190	0.093
ME	0.167	2.615	0.356
Lo	-1.906	-0.122	-0.802
LoP	0.000	-2.417	-0.287
OG	-0.224	-0.451	0.412
La	1.626	-0.517	0.591
AOTu	-0.570	-0.232	0.369
AL	-1.117	-0.565	0.296
MB-ca	-0.467	0.238	1.950
MB-lo+pe	-0.074	0.353	-0.935
CB	0.860	-0.619	-0.777
PB	0.755	0.741	0.726
POTu	-0.311	0.472	0.161

B) Discrimant function statistics

Correct group assignment		87%	
Eignevalue	3.090	2.065	0.528
% of variance	54.400	36.300	9.300
Wilks' Lambda	0.052	0.214	0.655
$\chi 2$	70.855	37.047	10.169
p	0.004	0.074	0.601

C) MANOVA statistics

F1(Species)	97.2632***	0.550	1.491
F1(Group)	4.6411*	11.695***	15.546***
F1(Species*Group)	0.000	38.172***	1.184

Table 6

A) Midbrain only

	Loadings	
	Residuals	
Neuropil	PC1	PC2
Antennal lobe	-0.981	-0.045
CB L+U	-0.798	0.406
MB Calyx	0.962	0.11
MB lobes+peduncle	0.952	0.231
AOTu	-0.047	0.966

B) Whole neuropil

	Loadings	
	Residuals	
Neuropil	PC1	PC2
Antennal lobe	0.761	0.619
CB L+U	0.671	0.67
MB Calyx	-0.961	0.212
MB lobes+peduncle	-0.942	0.222
AOTu	0.811	0.024
Medulla	0.042	-0.949
Lobula	0.92	-0.354
Lobula plate	0.962	-0.167

Table 6

A) Midbrain only

	Loadings	
	Residuals	
Neuropil	PC1	PC2
Antennal lobe	-0.981	-0.045
CB L+U	-0.798	0.406
MB Calyx	0.962	0.11
MB lobes+peduncle	0.952	0.231
AOTu	-0.047	0.966

B) Whole neuropil

	Loadings	
	Residuals	
Neuropil	PC1	PC2
Antennal lobe	0.761	0.619
CB L+U	0.671	0.67
MB Calyx	-0.961	0.212
MB lobes+peduncle	-0.942	0.222
AOTu	0.811	0.024
Medulla	0.042	-0.949
Lobula	0.92	-0.354
Lobula plate	0.962	-0.167

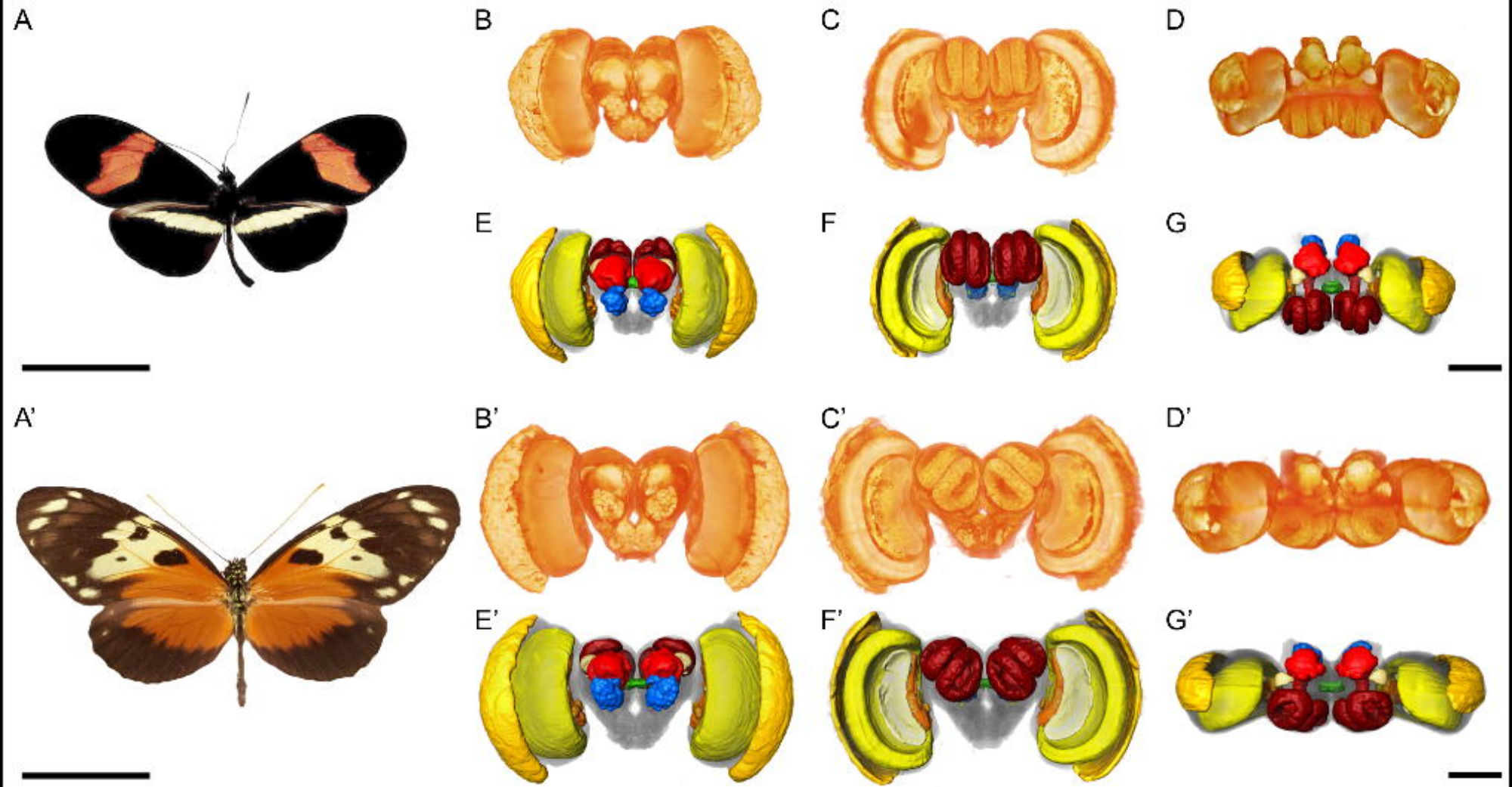
A
B
C
D
E
F
G
A'
B'
C'
D'
E'
F'
G'

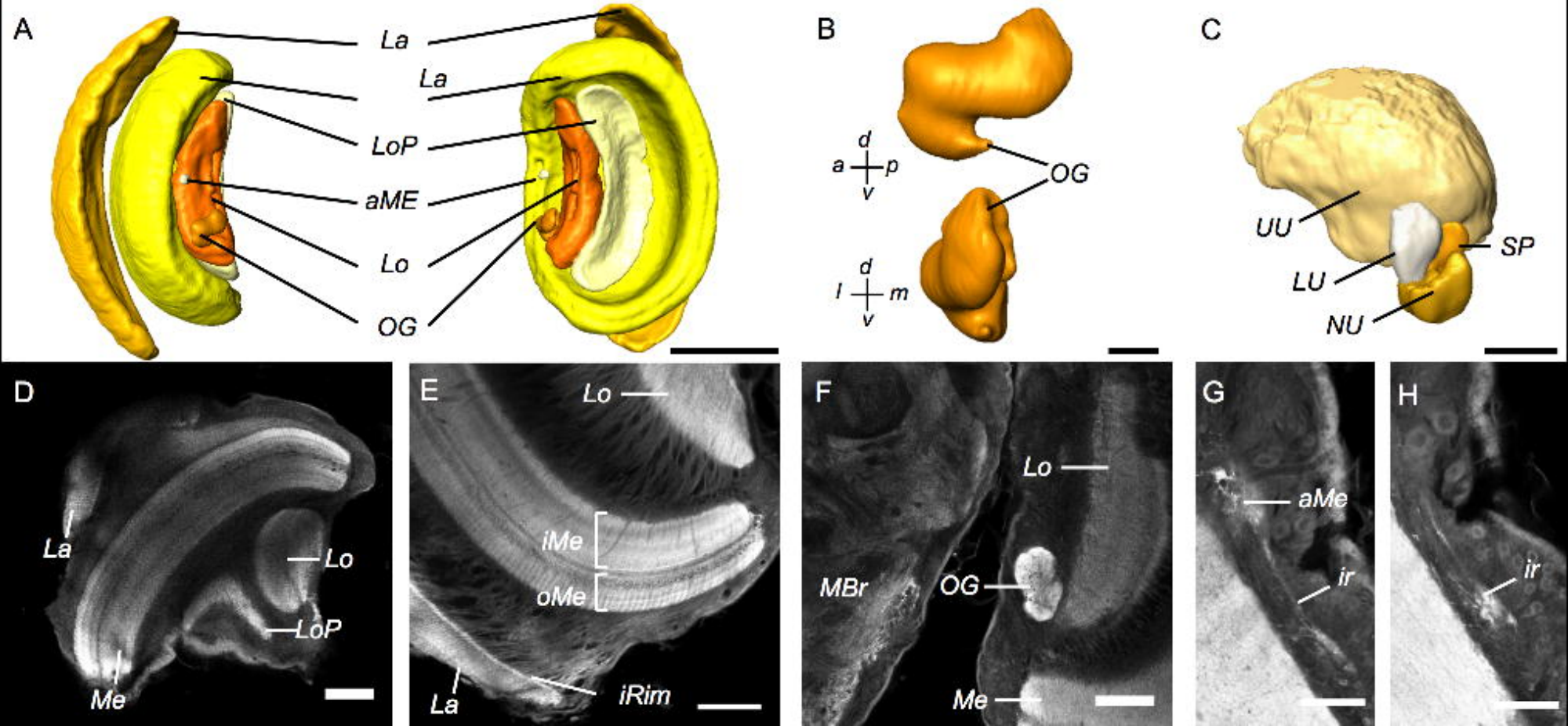
A
La
La
LoP
aME
Lo
OG
B
d
a
p
v
OG
d
l
m
v
C
UU
SP
LU
NU
D
La
Lo
LoP
Me
E
Lo
iMe
oMe
La
iRim
F
Lo
MBr
OG
Me
G
aMe
ir
H
ir

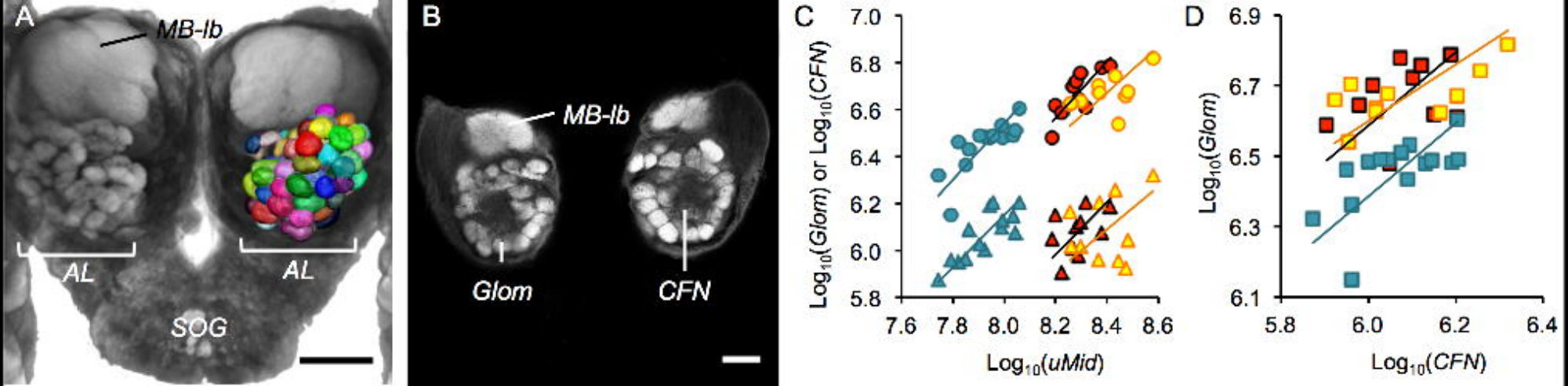
A
MB-lb
AL
AL
SOG
B
MB-lb
Glom
CFN
C
7.0
6.8
6.6
6.4
6.2
6.0
5.8
Log10(Glom) or Log10(CFN)
7.6
7.8
8.0
8.2
8.4
8.6
Log10(uMid)
D
6.9
6.7
6.5
6.3
6.1
Log10(Glom)
5.8
6.0
6.2
6.4
Log10(CFN)

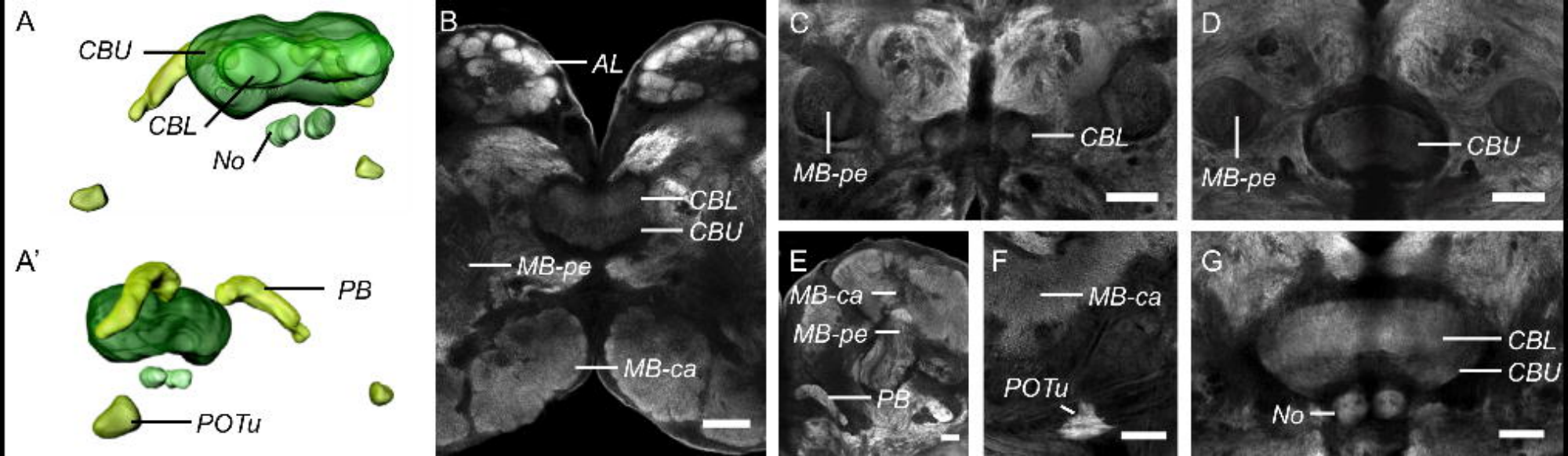
A
CBU
CBL
No
A'
PB
POTu
B
AL
CBL
CBU
MB-pe
MB-ca
C
CBL
MB-pe
D
CBU
MB-pe
E
MB-ca
MB-pe
PB
F
MB-ca
POTu
G
CBL
CBU
No

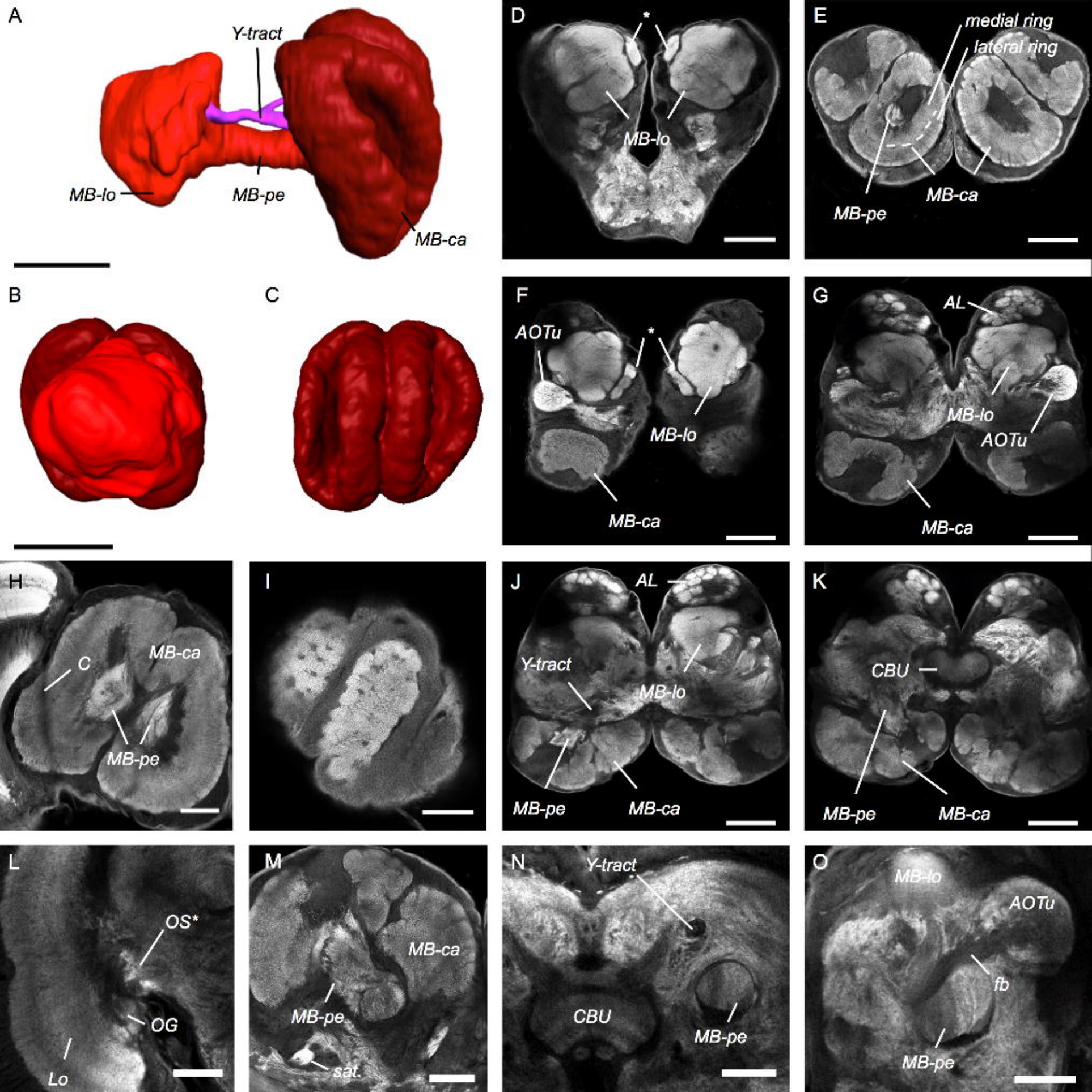
A
Y-tract
MB-lo
MB-pe
MB-ca
B
C
D
*
MB-lo
E
medial ring
lateral ring
MB-pe
MB-ca
F
AOTu
*
MB-lo
MB-ca
G
AL
MB-lo
AOTu
MB-ca
H
C
MB-ca
MB-pe
I
J
AL
Y-tract
MB-lo
MB-pe
MB-ca
K
CBU
MB-pe
MB-ca
L
OS*
OG
Lo
M
MB-ca
MB-pe
sat.
N
Y-tract
CBU
MB-pe
O
MB-lo
AOTu
fb
MB-pe

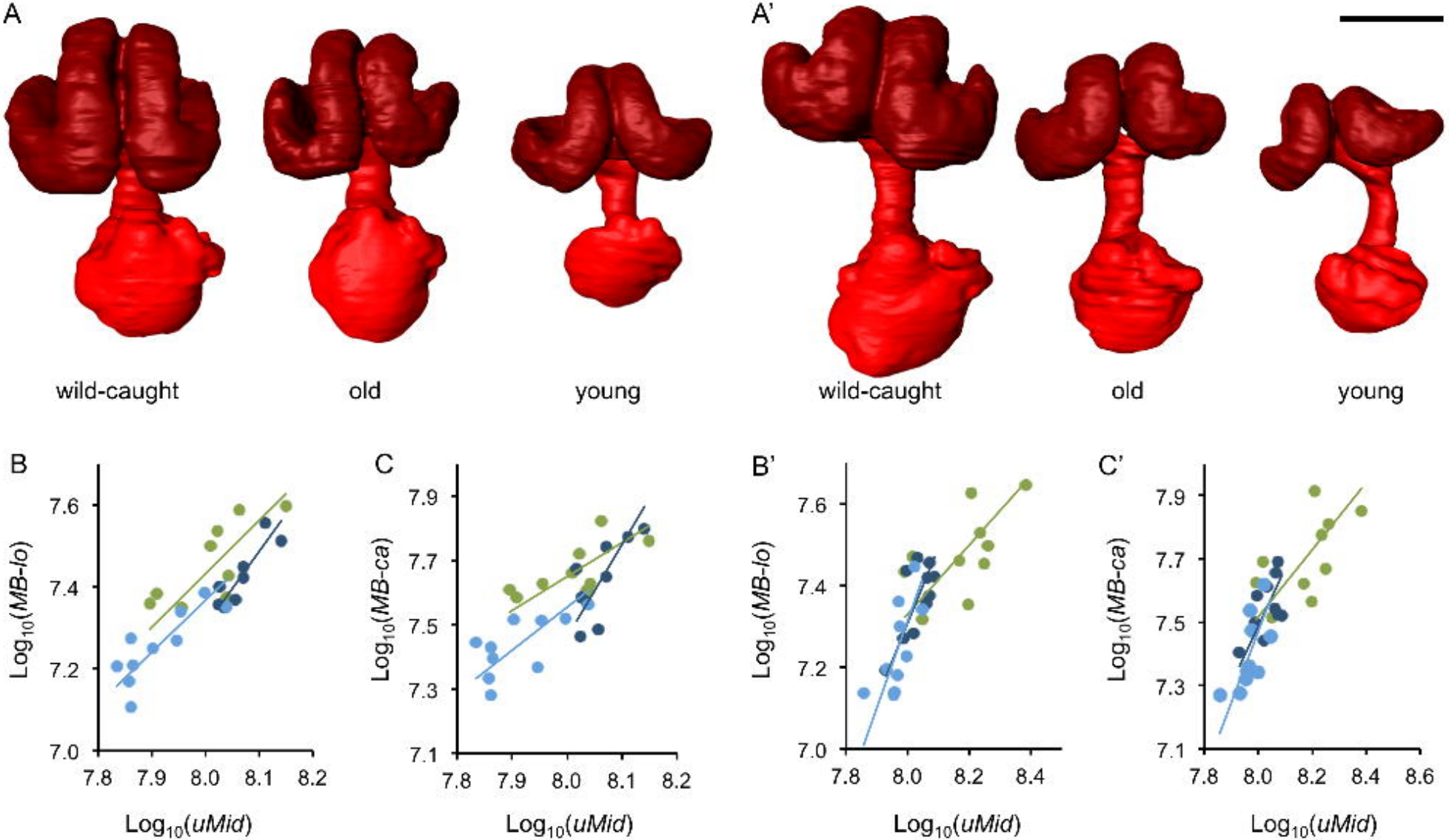
A
A'
wild-caught
old
young
wild-caught
old
young
B
C
B'
C'
Log10(MB-lo)
Log10(MB-ca)
Log10(uMid)
7.0
7.2
7.4
7.6
7.1
7.3
7.5
7.7
7.9
7.8
7.9
8.0
8.1
8.2
8.4
8.6

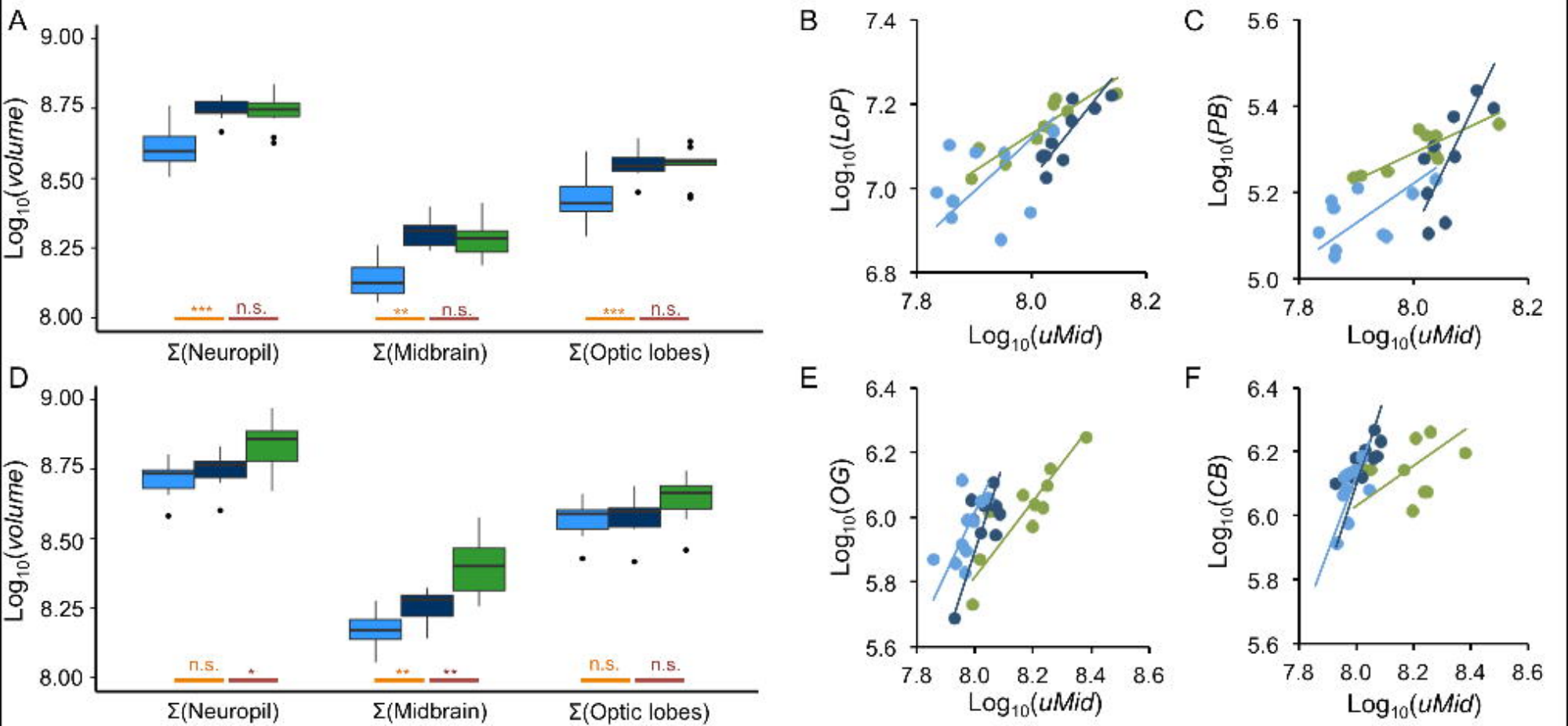
A
B
C
D
E
F
Log10(volume)
9.00
8.75
8.50
8.25
8.00
***
n.s.
**
n.s.
***
n.s.
Σ(Neuropil)
Σ(Midbrain)
Σ(Optic lobes)
n.s.
*
**
**
n.s.
n.s.
Log10(LoP)
7.4
7.2
7.0
6.8
7.8
8.0
8.2
Log10(uMid)
Log10(PB)
5.6
5.4
5.2
5.0
Log10(OG)
6.4
6.2
6.0
5.8
5.6
8.4
8.6
Log10(CB)

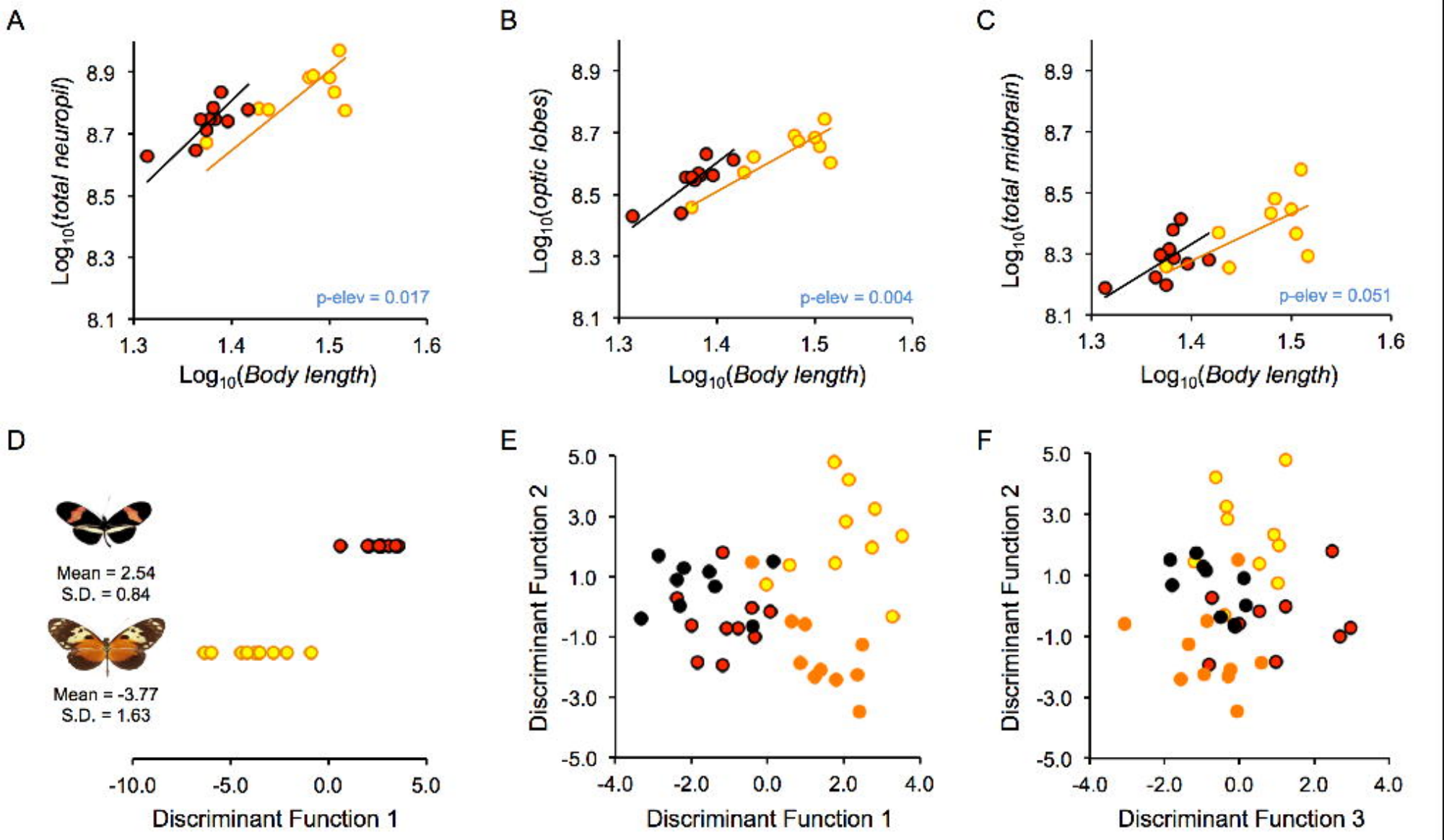
A
Log10(total neuropil)
8.9
8.7
8.5
8.3
8.1
1.3
1.4
1.5
1.6
Log10(Body length)
p-elev = 0.017
B
Log10(optic lobes)
8.9
8.7
8.5
8.3
8.1
1.3
1.4
1.5
1.6
Log10(Body length)
p-elev = 0.004
C
Log10(total midbrain)
8.9
8.7
8.5
8.3
8.1
1.3
1.4
1.5
1.6
Log10(Body length)
p-elev = 0.051
D
Mean = 2.54
S.D. = 0.84
Mean = -3.77
S.D. = 1.63
-10.0
-5.0
0.0
5.0
Discriminant Function 1
E
Discriminant Function 2
5.0
3.0
1.0
-1.0
-3.0
-5.0
-4.0
-2.0
0.0
2.0
4.0
Discriminant Function 1
F
Discriminant Function 2
5.0
3.0
1.0
-1.0
-3.0
-5.0
-4.0
-2.0
0.0
2.0
4.0
Discriminant Function 3

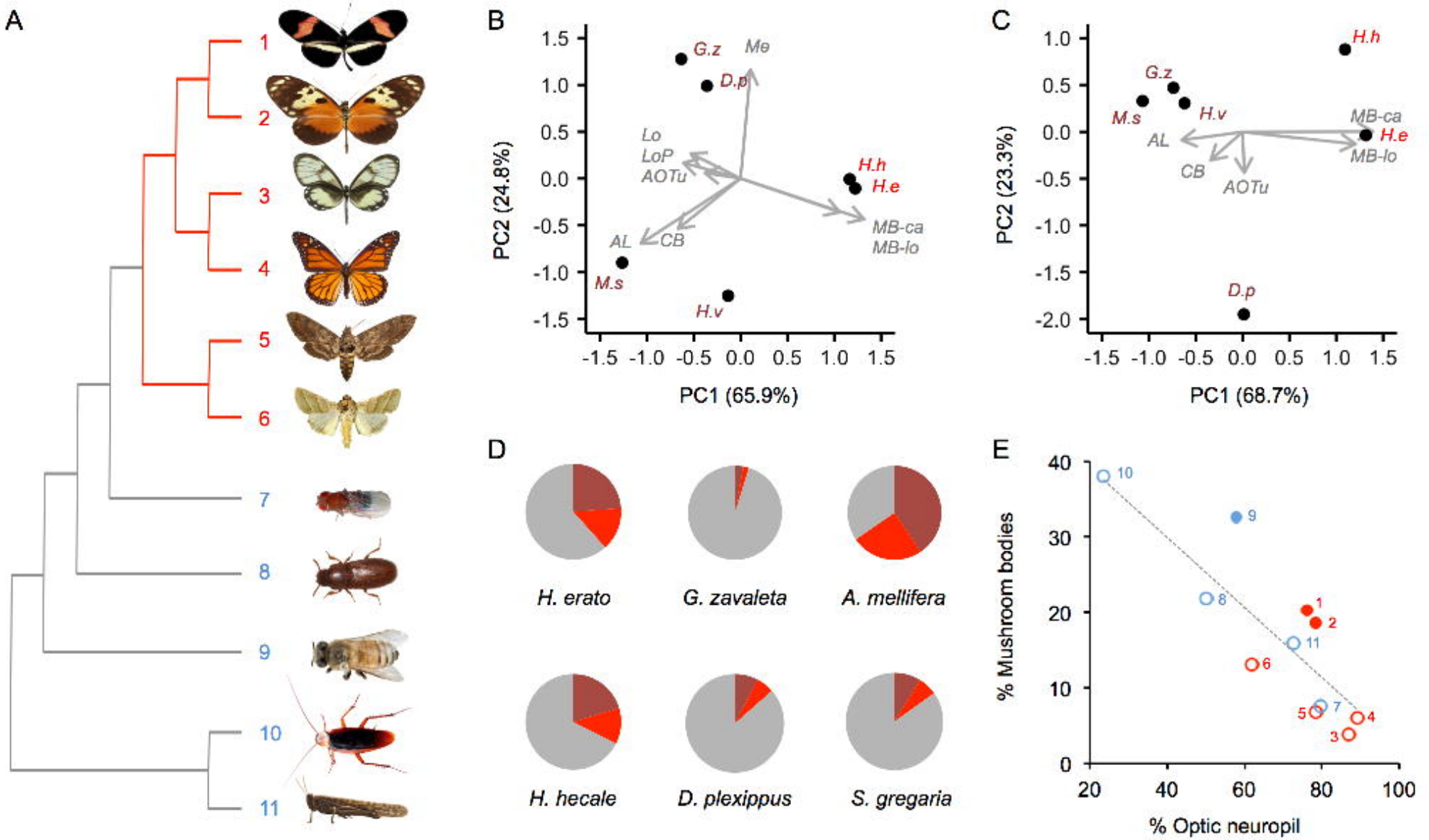
A
1
2
3
4
5
6
7
8
9
10
11
B
G.z
Me
D.p
Lo
LoP
AOTu
H.h
H.e
MB-ca
MB-lo
AL
CB
M.s
H.v
PC2 (24.8%)
PC1 (65.9%)
C
H.h
G.z
M.s
H.v
MB-ca
H.e
MB-lo
AL
CB
AOTu
D.p
PC2 (23.3%)
PC1 (68.7%)
D
H. erato
G. zavaleta
A. mellifera
H. hecale
D. plexippus
S. gregaria
E
% Mushroom bodies
% Optic neuropil